Symbiosis, hybridization and speciation in Mediterranean octocorals (Octocorallia, Eunicellidae)

Didier Aurelle[1,2*], Anne Haguenauer[3], Marc Bally[1], Frédéric Zuberer[4], Dorian Guillemain[4], Jean-Baptiste Ledoux[5], Stéphane Sartoretto[6], Cédric Cabau[7], Rachel Lapeyre[8], Lamya Chaoui[9], Hichem Kara[9], Sarah Samadi[2], Pierre Pontarotti[10,11,12]

[1] Aix Marseille Univ, Université de Toulon, CNRS, IRD, MIO, Marseille, France
[2] Institut Systématique Evolution Biodiversité (ISYEB), Muséum national d'Histoire naturelle, CNRS, Sorbonne Université, EPHE, Université des Antilles, CP 26, 75005 Paris, France.
[3] CNRS - Délégation Provence et corse, Marseille, France
[4] Aix Marseille Univ, CNRS, IRD, INRAE, OSU Inst. PYTHEAS, Marseille, France
[5] CIIMAR/CIMAR, Centro Interdisciplinar de Investigação Marinha e Ambiental, Universidade do Porto, Porto, Portugal.
[6] Ifremer, LITTORAL, 83500 La Seyne-sur-Mer, France
[7] Sigenae, GenPhySE, Université de Toulouse, INRAE, ENVT, 31326, Castanet Tolosan, France.
[8] MGX-Montpellier GenomiX, Univ. Montpellier, CNRS, INSERM, Montpellier France
[9] Laboratoire Bioressources marines. Université d'Annaba Badji Mokhtar, Annaba - Algérie.
[10] Aix Marseille Univ, MEPHI, Marseille, France.
[11] IHU Méditerranée Infection, Marseille, France.
[12] CNRS SNC5039

*Corresponding author
Correspondence: didier.aurelle@univ-amu.fr

ABSTRACT

Understanding how species can form and remain isolated in the marine environment still stimulates active researches. Here we study the differentiation and the possibility of hybridization among three temperate octocorals: *Eunicella cavolini*, *E. singularis* and *E. verrucosa*. Morphologically intermediate individuals have been observed between them. Among these three species, *E. singularis* is the only one described in mutualistic symbiosis with photosynthetic Symbiodiniaceae. The symbiosis between Symbiodiniaceae and scleractinian corals is well studied, especially in the context of the response to anthropogenic climate change. Nevertheless, the potential role of symbiotic interactions in speciation processes remains unknown in cnidaria. We tested here the possibility of hybridization between symbiotic and non-symbiotic *Eunicella* species. Through multivariate analyses and hybrid detection, we prove the existence of on-going gene flow between *E. singularis* and *E. cavolini*, with the observation of F1 and F2 hybrids, and backcrosses. Demographic inferences indicate a scenario of secondary contact between these two species. Despite current gene flow, these two species appear genetically well differentiated. Our data also suggest an intermediate abundance of Symbiodiniaceae in the hybrids of the two parental populations. We discuss the evolution of the Symbiodiniaceae / cnidarian symbiosis in the light of our results.

Keywords: speciation, hybridization, symbiosis, transcriptome, RAD sequencing, octocoral

1 Introduction

2

3 As corner stones of evolutionary biology, species and speciation still raise a wealth of
4 questions fuelled by the technological and conceptual advancements in genomics. Genomic
5 data allow testing hypotheses about species boundaries and origins. Named species are
6 indeed hypotheses, built on available data, that can be rejected or validated through the
7 integration of additional data and / or the use of additional criteria based on evolutionary
8 concepts (Pante *et al.*, 2015b). Sound species delimitations are useful, among others, to
9 better estimate species range and biodiversity patterns (Muir *et al.*, 2022; Coelho *et al.*,
10 2023), to avoid biases in studies of connectivity (Pante et al., 2015b), and of adaptive
11 abilities (Brener-Raffalli *et al.*, 2022). However, proposing sound species delimitation can be
12 problematic because different delimitation criteria may bring contradictory conclusions about
13 species boundaries (the Grey Zone of de Queiroz, 2007). This grey zone corresponds to
14 puzzling cases such as the absence of gene flow among morphologically undifferentiated
15 sets of organisms (i.e. cryptic species, Cahill *et al.*, 2024), or conversely, the detection of
16 gene flow among sets of organisms recognized, based on morphological distinctiveness, as
17 distinct species (Leroy *et al.*, 2020). Evolutionary inferences, based on genomic data, allow
18 testing scenarios of speciation and current gene flow: this provides a better understanding
19 on the origin and persistence of species at the light of genomic divergence (Roux *et al.*,
20 2016; De Jode *et al.*, 2023).

21 In the marine realm, the question of speciation is considered as particularly confusing.
22 Notably, how new species can originate from populations with large effective size associated
23 to high level of gene flow is still abundantly debated in the literature (e.g. Palumbi, 1992;
24 Mayr, 2001; Faria *et al.*, 2021). Difficulties in sampling and rearing organisms also hamper
25 experiments to test reproductive isolation (Faria *et al.*, 2021). Important progresses in
26 methodologies now allow to better understand spatial patterns of genetic structure in marine
27 organisms, for example through the study of oceanographic connectivity (Reynes *et al.*,
28 2021), clines in allele frequencies (Gagnaire *et al.*, 2015), and hybrid zones (Bierne *et al.*,
29 2003).

30 In this context, the role of symbiotic interactions in reproductive isolation remains poorly
31 investigated. There are various examples of the involvement of microbial species in
32 reproductive isolation, especially in insects (Brucker and Bordenstein, 2012). For marine
33 species, microbial communities have been mainly explored in light of adaptative evolution
34 (Rosenberg and Zilber-Rosenberg, 2018). Shallow water scleractinian corals (hexacorals)
35 are usually associated with various species of photosynthetic zooxanthellae, in the family
36 Symbiodiniacae (Cairns, 2007; LaJeunesse *et al.*, 2018). Changes in associated
37 Symbiodiniaceae can impact the thermotolerance of the coral holobiont, and the possibility

of adaptation facing climate change (Berkelmans and van Oppen, 2006; van Oppen & Medina, 2020). Inferences from the phylogeny of Anthozoans (hexacorals and octocorals) have shown multiple acquisitions of the symbiotic state throughout evolution (Cairns, 2007; Campoy *et al.*, 2020, Mc Fadden *et al.*, 2021). The symbiotic interactions between Anthozoans and Symbiodiniaceae provide important mutualistic benefits especially from a nutritional point of view (Furla *et al.*, 2005). These interactions require specific adaptations for the animal host, as for example protection against oxygen produced by photosynthesis (Furla *et al.*, 2005). Therefore, one can hypothesize that in hybrids such adaptations could be modified and a breakdown of symbiosis could occur, leading to reduced fitness. The association with Symbiodiniaceae can range from mutualism to parasitism (Sachs and Wilcox, 2006; Lesser *et al.*, 2013; see also Matz, 2024), and a change in the genomic background in hybrid hosts could modify the nature of symbiosis as well. The presence of Symbiodiniaceae could then be involved in genetic incompatibilities with the host genome, as previously observed with bacterial species (Bordenstein, 2003; Brucker and Bordenstein, 2012). All these observations raise the question of the potential role of Symbiodiniaceae in speciation and reproductive isolation in Anthozoans. This topic has been poorly explored up to now. In *Plexaura* octocorals, two incompletely isolated species have been shown to present different populations of Symbiodiniaceae, questioning their role in species boundaries (Pelosi *et al.*, 2020).

Here we explore the robustness of species limits between named species of the gorgonian genus *Eunicella* (Octocorallia, Eunicellidae) documented as displaying different symbiotic relationships. In shallow conditions (above 50 m depth), three *Eunicella* species are mainly present in the Mediterranean Sea: *Eunicella cavolini* (Koch, 1887), *E. singularis* (Esper, 1971), and *E. verrucosa* (Pallas, 1766). These three species have partially overlapping ranges, and they can be observed in sympatry in the area of Marseille (France). *Eunicella singularis* hosts Symbiodiniaceae corresponding to the *Philozoon* genus (Forcioli *et al.*, 2011; LaJeunesse *et al.*, 2018, 2022; Porro, 2019), whereas the two other gorgonian species are devoided of these symbionts (Carpine and Grasshoff, 1975). The Symbiodiniaceae contribute to the carbon metabolism of *E. singularis*, but a non-symbiotic *aphyta* morph has already been observed (Gori *et al.*, 2012). The lack of variability in mitochondrial DNA does not allow to distinguish these three species (Calderón *et al.*, 2006), and a study using two nuclear introns suggested the possibility of hybridization between *E. cavolini* and *E. singularis* (Aurelle *et al.*, 2017). Moreover, demographic inferences based on a large number of nuclear loci in *E. cavolini* and *E. verrucosa* indicated the possibility of current gene flow between these two species (Roux *et al.*, 2016). However, these data are incomplete because neither individuals identified as *E. singularis*, nor individuals that are morphologically difficult to attribute to a named species (potential hybrids) have been

75 analysed. Here, we will go further on these topics with the following objectives: i) estimate
76 the genomic differentiation among these three species and test for species limits, ii) test
77 whether symbionts are present or absent in the hybrids, to look for a possible breakdown in
78 symbiosis, and iii) infer scenarios of speciation. Studying the history of speciation is useful to
79 infer how divergence happened, and to test the possibility of current and past gene flow.
80 Analysing the hybrid status on morphologically intermediate individuals allows to further test
81 if hybridization is still on-going. We used restriction sites associated DNA sequencing (RAD-
82 sequencing; Baird *et al.*, 2008) to test species limits and hybridization. We complementary
83 used transcriptome data for demographic inferences, for the analysis of putative hybrids, and
84 to test for the presence of Symbiodiniaceae. The results will be useful to better understand
85 the evolution of these species in different environments and particularly the possible impact
86 of hybridization in adaptation to changing environment.
87
88 **Material and methods**
89
90 **Species distribution**
91
92   *Eunicella verrucosa* is present both in the Eastern Atlantic Ocean and the Mediterranean
93 Sea (Carpine and Grasshoff, 1975). In the Atlantic, *E. verrucosa* can be found from Ireland
94 and West coasts of Britain, to Angola (Grasshoff, 1992; Readman and Hiscock, 2017).
95 *Eunicella verrucosa* has been observed in the North Western Mediterranean Sea, in
96 Sardinia (Canessa et al., 2022), and in the Adriatic and Aegean Seas (Chimienti, 2020). In
97 the Mediterranean Sea, *E. verrucosa* can be observed from shallow conditions (20-40 m) up
98 to 200 m depth (Sartoretto and Francour, 2011; Fourt and Goujard, 2012; Chimienti, 2020).
99 *Eunicella singularis* and *E. cavolini* are only present in the Mediterranean Sea. *Eunicella*
100 *cavolini* can be observed in the Western Mediterranean, Adriatic and Aegean Seas, from 5 to
101 200 m depth (Sini *et al.*, 2015; Carugati *et al.*, 2022). *Eunicella singularis* can be found in the
102 Western Mediterranean and Adriatic Seas, and, less frequently, in the Eastern
103 Mediterranean (Gori *et al.*, 2012). It is usually observed up top 40 m depth. *Eunicella*
104 *singularis* is the only Mediterranean octocoral known to harbour Symbiodiniaceae (but see
105 Bonacolta *et al.*, 2024). These Symbiodiniaceae belong to the temperate clade A (Forcioli *et*
106 *al.*, 2011; Casado-Amezúa *et al.*, 2016), now corresponding to the *Philozoon* genus
107 (LaJeunesse *et al.*, 2018, 2022). Deep occurrences (up to 70 m) of *E. singularis* have been
108 mentioned, and assigned to the *aphyta* morph, without Symbiodiniaceae (Gori et al., 2012).
109 In the area of Marseille, these three species can be observed in sympatry and at the same
110 depth (Sartoretto and Francour, 2011).
111

Sampling

The sampling for RAD sequencing included 25 specimens identified as *E. cavolini*, 23 *E. singularis*, seven *E. verrucosa*, and 12 morphologically intermediate individuals (potential hybrids). These latter individuals displayed intermediate colors and branching patterns between *E. cavolini* and *E. singularis (*Figure S1), and they were analysed to test their hybrid status (Aurelle *et al.*, 2017). The specimens have been sampled by scuba diving at different periods in the area of Marseille, where the three species are present in sympatry (Figure S2; Table S1).

For transcriptome sequencing, specimens attributed to *E. cavolini*, *E. singularis*, and *E. verrucosa* have been collected in the Mediterranean (for the three species), and in the Atlantic (*E. verrucosa* only; Table S2; Figure 1) in 2016. The final sampling for transcriptomics included five *E. cavolini*, eight *E. singularis*, three *E. verrucosa*, and four potential hybrids.

Sampling was non-destructive, with authorizations from the local authorities, including Marine Protected Areas.

Mitochondrial MutS

To test the genetic proximity of three *Eunicella* species studied here, we built a tree with mitochondrial MutS sequences (McFadden *et al.*, 2011), available in GenBank. The methods and sequences are detailed in supplementary Figure S3, and Table S3.

RAD sequencing

DNA has been extracted with the Macherey-Nagel NucleoSpin DNA RapidLyse kit. RAD library preparation (with the PstI restriction enzyme) and sequencing (Illumina NovaSeq600 with 150 nucleotides paired-end sequencing) have been performed at the MGX platform (CNRS). The MGX platform performed control quality, demultiplexing and removal of PCR duplicates with unique molecule identifiers. Potential contaminants have been removed with kraken2 (Wood *et al.*, 2019; Lu *et al.*, 2022). RAD loci have been assembled with ipyrad (Eaton and Overcast, 2020). We tested four assembly strategies to test the robustness of the results: a *de novo* assembly, with a clustering threshold of 0.85, and assembly on a reference genome, with each of the three available genomes: for *E. cavolini*, *E. singularis*, and *E. verrucosa* (Ledoux *et al.*, in prep).

 From these datasets, we built four datasets focused on the differentiation between *E. cavolini* and *E. singularis*: we excluded *E. verrucosa* samples and we retained the first

149 percent of the loci with the highest F_{ST} between *E. cavolini* and *E. singularis*. These last
150 datasets will be labelled as "1%" (see characteristics of the different datasets are
151 summarised in Table S4).
152

Transcriptome sequencing and SNPs calling

155 Total RNA has been extracted as in Haguenauer *et al.* (2013). RNAs were sent to the LIGAN
156 genomic platform for sequencing (Lille, France) on four flow cells of Illumina NextSeq 500
157 (2 x 75 bp). The transcriptomes have been assembled with the *de novo* RNA-Seq Assembly
158 Pipeline (DRAP ; Cabau *et al.*, 2017) with Oases (Schulz *et al.*, 2012) and default
159 parameters. We performed an individual assembly, and a meta-assembly to be used as
160 reference. The statistics describing the assembled transcriptomes are given in Table S2. We
161 used the BLAT software (Kent, 2002) and the blat_parser.pl script to remove potential
162 Symbiodiniaceae sequences in the obtained transcriptomes, with the transcriptome of the
163 type A1 (Baumgarten *et al.*, 2013) as a reference.
164 We mapped the reads on the meta transcriptome filtered for Symbiodiniaceae sequences
165 with bwa option mem (Li and Durbin, 2009). The obtained sam files were converted in bam
166 format with samtools 1.9 (Li *et al.*, 2009), and sorted with Picard tools ('Picard Toolkit', 2019).
167 The SNPs calling has been performed with reads2snp 2.0 with default parameters
168 (Tsagkogeorga *et al.*, 2012; Gayral *et al.*, 2013). The obtained dataset, including variable
169 and non variable sites, will thereafter be referred as the "all sites" dataset. We performed
170 separate SNP calls with reads2snp for pairwise comparisons among species and without the
171 potential hybrid samples. These three datasets have been used for demographic inferences,
172 and will be referred as "all-CS" for the *E. cavolini* / *E. singularis* comparison, "all-CV" for
173 the *E. cavolini* / *E. verrucosa* comparison, and "all-SV" for the *E. singularis* / *E.
174 verrucosa* comparison.
175 For an analysis of genetic differentiation, we filtered the "all sites" vcf file with vcftools
176 (Danecek *et al.*, 2011). We retained biallelic sites, without missing data, and separated by at
177 least 1 kb: this is the "polymorphic sites" dataset. As for RAD sequencing, we built a dataset
178 focused on the differentiation between *E. cavolini* and *E. singularis*, retaining the 1% loci with
179 the highest differentiation between *E. cavolini* and *E. singularis* (Table S4).
180

Presence of Symbiodiniaceae

183 We analysed the presence of Symbiodiniaceae in *Eunicella* gorgonians with transcriptome
184 data. First, we counted the number of reads corresponding to the Symbiodiniaceae
185 transcriptome type A1 with Salmon (Patro *et al.*, 2017). Second, we used the percentage of

186 assembled sequences (contigs) in the *Eunicella* transcriptomes corresponding to
187 Symbiodiniaceae following the BLAT analysis. We used a Kruskal-Wallis test in R to test for
188 differences among the four groups of samples (the three *Eunicella* species and the potential
189 hybrids) for each metric. Additionally, we performed a BLAST analysis with the LSU, ITS and
190 psbA sequences of *Philozoon* (LaJeunesse *et al.*, 2022) to try to identify the
191 Symbiodiniaceae genera present in the different samples.

192 As our data pointed to the unexpected presence of Symbiodiniaceae in *E. cavolini* (see
193 Results), we further explored this topic with preliminary data from another experiment
194 dedicated to studying the microbiome of *E. cavolini* and *E. singularis*. This pilot study
195 involved an analysis of microeukaryotic communities through 18S rDNA metabarcoding on
196 two colonies of *E. cavolini*, and one *E. singularis (*Supplementary File S2).

197

198 **Genetic differentiation and analysis of hybrids**

199

200 With RAD sequencing data, we performed the analysis of genetic diversity with the four
201 datasets including all loci. With transcriptomes, we performed the same analyses with the
202 "polymorphic sites" dataset. We used the LEA R package to estimate ancestry coefficients
203 (Frichot *et al.*, 2014; Frichot and François, 2015). We tested K values from 1 to 10, with 10
204 replicates for each K. To analyse the genetic differences among individuals, we performed a
205 Principal Component Analysis (PCA) with the R package adegenet (Jombart, 2008). The
206 pairwise F_{ST} (Weir and Cockerham, 1984) estimated among species were computed with the
207 R package Genepop (Rousset, 2008; Rousset *et al.*, 2020), after conversion of the vcf file
208 with PGDSpider (Lischer & Excoffier, 2012). The distribution of F_{ST} among loci was obtained
209 with vcftools.

210 The hybrid status (e.g. first generation hybrids) of morphologically intermediate individuals
211 was analysed with the NewHybrids software (Anderson and Thompson, 2002). We used the
212 genepopedit R package to prepare the input file from genepop format (Stanley *et al.*, 2017).
213 Following the results of the LEA and PCA analyses, we compared *E. cavolini*, *E. singularis*
214 and potential hybrids. The NewHybrids analysis has difficulties to converge with a high
215 number of loci compared to the number of individuals
216 (https://github.com/eriqande/newhybrids/issues/5). We therefore used the different "1%
217 SNP" datasets of RAD sequencing and transcriptome datasets (i.e. the most differentiated
218 loci) for the NewHybrids analysis. As a prior, we used individuals with the lowest levels of
219 admixture in LEA as potential parental individuals. For the RAD datasets, this corresponded
220 to ten individuals of each species as priors. For transcriptome sequencing this corresponded
221 to three individuals for *E. cavolini*, and six individuals for *E. singularis*. Each NewHybrids
222 analysis was repeated ten times to test the robustness of the results.

223

Scenarios of speciation

226 We tested scenarios of speciation with the Demographic Inferences with Linked Selection
227 (DILS) pipeline (Csilléry, *et al.*, 2012; Pudlo *et al.*, 2016; Fraïsse *et al.*, 2021) on
228 transcriptome data only. Note that with the high number of loci recovered with
229 transcriptomes, the numbers of specimens used here are adequate for robust inferences
230 (Roux *et al.*, 2016). The DILS pipeline allows the analysis of two species scenarios only: we
231 therefore performed separate analyses for the three two-species comparisons, with the "all-
232 CS", "all-CV", and "all-SV" pairwise datasets. We did not include the potential hybrids in the
233 analysis, which would have required the consideration of a separate population. The tested
234 scenarios are presented in Figure S4 (see Fraïsse *et al.*, 2021 for details). Briefly, DILS
235 allows testing scenario with current migration (i.e. gene flow), such as isolation / migration or
236 secondary contact, versus scenarios of current isolation (no gene flow), such as complete or
237 ancestral migration (gene flow among ancestral populations).
238 We used the same priors for all analyses, with different numbers of sequences per gene and
239 per sample according to the dataset (Table S5). For all pairwise comparisons, we performed
240 two DILS analyses: one with constant population sizes, and one with variable population
241 sizes.

242

Results

244

Mitochondrial MutS

246

247 The mitochondrial MutS sequences available in GenBank confirmed the proximity of the
248 three *Eunicella* species analysed here: all sequences were identical for these three species,
249 as well as for three other sequences deposited in GenBank as unidentified *Eunicella* (Figure
250 S3). The closest species to this group was *Eunicella racemosa*. All other *Eunicella* MutS
251 sequences (*E. tricoronata* and *E. albicans*) grouped separately with *Complexum monodi*, but
252 with low bootstrap support.

253

Presence of Symbiodiniaceae

255

256 The transcriptomes showed low numbers of reads counts aligning on the Symbiodiniaceae
257 transcriptome (1868 to 58406 reads; Table S6). The proportion of contigs corresponding to
258 Symbiodiniaceae with BLAT was also very low (between 0.00276 and 0.03686; Table S6).
259 Significant differences were observed among species in both cases (Kruskal-Wallis test, p =

260   0.047 for reads counts, and p = 0.002 for the proportions of contigs). The pairwise Wilcoxon-
261   Test showed significant differences only for the comparisons of proportions of contigs
262   involving *E. singularis*, which was higher than in other species (Table S7; Figure 2). The
263   mean values of reads counts and contigs for the Symbiodiniaceae in the hybrids were lower
264   than in *E. singularis* and *E. cavolini* but higher than in *E. verrucosa*, although pairwise tests
265   were not significant.
266   The BLAST analysis with the LSU, ITS and psbA sequences of *Philozoon* only retrieved
267   corresponding sequences in the transcriptomes of *E. singularis*. Regarding the pilot study of
268   18S rDNA metabarcoding, a diversity of 92 Operational Taxonomic Units (OTUs)
269   corresponding to Symbiodiniaceae in the Silva database was observed in *E. singularis*, with
270   a single OTU largely dominant in abundance (Supplementary file S2). The same OTU was
271   also observed in *E. cavolini* with a low abundance of reads, but still representing 99% of all
272   12 to 13 Symbiodiniaceae OTUs detected in the two analysed colonies. A BLAST search in
273   GenBank identified a subset of Symbiodiniaceae sequences related to this OTU.
274   Phylogenetic inference based on these data indicated that this OTU was related to clade A of
275   the Symbiodiniaceae.
276
277   **Genetic differentiation and analysis of hybrids**
278   With RAD sequencing we obtained between 12 952 and 29 061 SNPs for the assembly on
279   *E. cavolini* and *E. verrucosa* genomes respectively (Table S4). The F_{ST} estimates from RAD
280   sequencing were highest for the comparisons between *E. verrucosa* and all other samples
281   (F_{ST} between 0.51 and 0.66 depending on dataset; Table S8). The F_{ST} between *E. cavolini*
282   and *E. singularis* was lower (F_{ST} between 0.29 and 0.38), and the lowest F_{ST} values were
283   observed for hybrids compared to these two species (F_{ST} between 0.09 and 0.13). The
284   cross-entropy analysis using LEA with RAD sequencing showed a minimum at K = 3 for the
285   four datasets (results not shown). The barplots of coancestry coefficients were very similar
286   for the four datasets, with a separation of the three species, and an admixture between
287   *E. cavolini* and *E. singularis* for the morphologically intermediate individuals (Figure S5). The
288   PCAs on RAD sequencing were very similar for all datasets, with a separation between
289   *E. verrucosa* and all other samples on the first axis (Figure S6). The second axis separated
290   *E. cavolini* and *E. singularis*, with the potential hybrids in intermediate position between
291   them. Projections on axes 3 and 4 resulted mainly in the separations *of E. verrucosa*
292   samples from each other.
293   With transcriptomes, we obtained 31 369 SNPs for the "polymorphic sites" dataset. With this
294   dataset, the highest F_{ST} values were observed for the comparisons between *E. verrucosa*
295   and all other samples ($F_{ST} > 0.43$; Table S9). The F_{ST} between *E. cavolini* and *E. singularis*
296   was much lower (0.21), and the lowest F_{ST} values were observed for hybrids compared to

297   these two species (F_{ST} around 0.07 in both cases). These differences corresponded to
298   different distributions of F_{ST} over SNPs (Figure S7). For the 1% SNPs with the highest F_{ST}
299   estimates, 52 SNPs were shared by both comparisons involving *E. cavolini* (i.e. *E. cavolini*
300   vs *E. singularis* and *E. cavolini* vs *E. verrucosa*), 116 top 1% SNPs were shared by both
301   comparisons involving *E. singularis*, and 1042 top 1% SNPs were shared by both
302   comparisons involving *E. verrucosa*.

303   The cross-entropy analysis using LEA with transcriptomes indicated a best clustering
304   solution corresponding to K = 2 or K = 3 clusters (Figure S8). At K = 2, the first distinction
305   was observed between *E. verrucosa* and all other samples (Figure 3). The K = 3 analysis
306   further separated *E. cavolini* and *E. singularis*, with morphologically intermediate individuals
307   admixed between these two species. Conversely the individuals representative of *E. cavolini*
308   and *E. singularis* presented low levels of admixture, apart from the *E. cavolini* of the site in
309   Algeria (code ANB), and, at a small level, two *E. singularis* individuals from Banyuls (BAN).
310   At K = 4, the two *E. cavolini* individuals from Algeria separated from other *E. cavolini* from
311   the northern part of the Mediterranean.

312   As with RAD sequencing, the PCA on transcriptome SNPs separated *E. verrucosa* from
313   other samples on the first axis (Figure 4). The second axis separated *E. cavolini* and
314   *E. singularis*, with the potential hybrids in intermediate position between them. The third axis
315   separated the *E. cavolini* samples from Algeria (ANB site) from all other samples (Figure
316   S6).

317   The NewHybrids analysis on RAD sequencing indicated that all morphologically intermediate
318   individuals, except one, appeared as hybrids: first generation (F1), second generation (F2),
319   or backcrosses with *E. singularis* or *E. cavolini* (Table 1). These samples also appeared
320   admixed on the basis of LEA (Figure S5). One individual identified as a potential hybrid *in*
321   *situ*, was inferred as a parental *E. singularis*. For four individuals, the hybrid status varied
322   according to the dataset: F2 or backcross with *E. cavolini* in two cases, F1 or F2 in two
323   cases. Potential parental individuals not included in the priors were well inferred as parental
324   with NewHybrids. The NewHybrids analysis with transcriptomes indicated that the
325   morphologically intermediate individuals were hybrids with a probability of one in all ten
326   iterations of the analysis. One individual was a F1 hybrid, another one was F2 hybrid, and
327   the two other ones corresponded to backcrosses with *E. singularis* (Figure 3; Table 1). In the
328   same analysis, the *E. cavolini* and *E. singularis* individuals not included as priors for parental
329   species (see Figure 3 for the individuals used as priors), were indeed inferred as parental
330   with a probability of one, including the *E. cavolini* individual from Algeria (ANB).

331

332   **Scenarios of speciation**

333

334 The average pairwise net divergence estimated from DILS was 0.0018 between *E. cavolini*

335 and *E. singularis,* and around 0.007 for the two comparisons with *E. verrucosa* (Table S9,

336).   The

337 DILS analysis indicated the existence of current gene flow between *E. cavolini* and

338 *E. singularis* with high probability, both with constant and variable population sizes (p = 0.87

339 and 0.88 respectively; Table 2). This possibility of gene flow corresponded to a scenario of

340 secondary contact. Conversely, a model of current isolation was inferred for the comparisons

341 between *E. verrucosa* and each of the two other species, with a probability p ≥ 0.87: in these

342 two cases, the inferred scenario included a period of ancestral migration, though with

343 moderate support (p between 0.61 and 0.69). A genomic heterogeneity in effective size (i.e.

344 variations among loci) was inferred with strong support (p ≥ 0.99) for all analyses. In the

345 case of current gene flow (between *E. cavolini* and *E. singularis*), a genomic heterogeneity in

346 migration rates was inferred (p ≥ 0.82). We repeated the DILS analysis without including the

347 two divergent samples of *E. cavolini* from Algeria: this led to similar results, with inference of

348 secondary contact for the comparison with *E. singularis*, and ancestral migration for the

349 comparison with *E. verrucosa* (results not shown). For parameters inferences, we used the

350 complete datasets, with all *E. cavolini* samples. The inferred parameters for the different

351 scenarios are presented in Supplementary Table S9. We will first present the results

352 obtained for the constant population sizes models. The divergence time between *E. cavolini*

353 and *E. singularis* (median 403 273 generations) was much lower than between *E. cavolini*

354 and *E. verrucosa* (median 1 054 488 generations)*,* and between *E. singularis* and

355 *E. verrucosa* (median 899 098 generations). For the comparison between *E. cavolini* and

356 *E. singularis,* the time of secondary contact was estimated after around 85% of time spent in

357 isolation since divergence. Following secondary contact, the gene flow was similar in both

358 directions for these two species. The duration of ancestral migration roughly corresponded to

359 6% and 8% of the total time since divergence for the comparison between *E. cavolini* and

360 *E. verrucosa*, and for the comparison between *E. singularis* and *E. verrucosa*, respectively.

361 For these last two cases, the gene flow (forward in time) during ancestral migration was

362 higher towards *E. verrucosa* than in the opposite direction. The estimated effective sizes

363 were of similar order for *E. cavolini* and *E. verrucosa*. Similar results were obtained for the

364 models including variations in effective size, except for the estimate of current gene flow

365 between *E. cavolini* and *E. singularis*: with variable population size, gene flow from

366 *E. singularis* to *E. cavolini* was higher than in the opposite direction.

367

368

369 **Discussion**

370

371   The three named *Eunicella* species studied here have been previously described with
372   differences in colony morphology, sclerites shape, and in the presence of photosynthetic
373   Symbiodiniaceae (Carpine and Grasshoff, 1975). Our results demonstrate a continuum
374   between *E. cavolini* and *E. singularis*, with morphologically intermediate individuals, on-going
375   gene flow, and hybrids characterised by a reduced frequency of Symbiodiniaceae compared
376   to *E. singularis*. On the other hand, *E. verrucosa* appears genetically isolated from these two
377   species. We will discuss here the differences observed among markers, the outcome of
378   hybridization, the speciation scenarios, and what can be learnt on the evolution of symbiosis.
379

380   **Discordances between molecular markers**

381

382   As previously observed (Aurelle *et al.*, 2017), mitochondrial DNA did not allow to discriminate
383   the three species due to the usually slow evolution of mitochondrial DNA in octocorals
384   (McFadden *et al.*, 2011; Muthye *et al.*, 2022). The use of transcriptome sequences first
385   confirmed the closer proximity between *E. cavolini* and *E. singularis* than with *E. verrucosa*.
386   This had been previously suggested with two intron sequences, but with incomplete lineage
387   sorting (Aurelle *et al.*, 2017). The Mediterranean *Eunicella* then add a new example of the
388   lack of power of mitochondrial DNA to discriminate genetically differentiated octocoral
389   species, as demonstrated in other genera (Erickson *et al.*, 2021; Pante *et al.*, 2015a). The
390   slow rate of evolution of mitochondrial DNA in octocorals has been linked to the presence of
391   the mitochondrial locus MutS, an homolog of a bacterial gene involved in DNA repair.
392   However, there are contradictory examples showing that the presence of this locus is not the
393   only factor explaining the slow evolution of mitochondrial DNA in octocorals (Muthye *et al.*,
394   2022). More generally, as hybridization can lead to the sharing of mitochondrial DNA among
395   species, the use of multiple independent nuclear loci is required for species discrimination in
396   such cases.

397

398   **Incomplete reproductive isolation among two named species**

399

400   Inferences of genetic ancestry and hybrid status confirmed that morphologically intermediate
401   individuals are indeed hybrids between *E. singularis* and *E. cavolini*, with the identification of
402   F1, F2 and backcrosses with both parental lineages: first generation hybrids can then be
403   fertile. The fact that gene flow indeed goes further than the hybrid levels is confirmed by the
404   DILS analysis, which did not include hybrid individuals. Reproductive isolation is therefore at
405   least partial between these lineages. The ease to find hybrids in the area studied here, as
406   well as similar observations in other sites (S. Sartoretto, pers. com.) indicate that
407   hybridization is not rare on an evolutionary scale. Similarly, transcriptome sequencing has

408 led to infer hybridization among *Plexaura* species on the basis of a small number of samples

409 (Pelosi *et al.*, 2022).

410 The alternation of populations with and without hybrids would point to a mosaic hybrid zone

411 (Bierne *et al.*, 2003), where hybrids could form in different areas and from different parental

412 populations. As, or because, hybridization between *E. cavolini* and *E. singularis* had not

413 been reported before, the presence of hybrids has probably been overlooked up to now. This

414 may be the consequence of previously focusing on colonies with "typical" morphologies. The

415 frequency of hybridization therefore remains to be studied.

416 Our results allow discussing the evolution of genomic divergence among these species. The

417 persistence of genomic differentiation between these lineages in sympatry, despite current

418 gene flow, indicates that intrinsic (i.e. genomic incompatibilities) or extrinsic (e.g. ecology)

419 factors can maintain partial isolation. Difference or overlap in the timing of reproduction

420 should also be considered in contributing to pre-mating isolation (Pelosi *et al.*, 2022). A

421 better characterization of the ecological range of parental and hybrid populations would be

422 useful to test if local adaptation is involved in their distribution. Intrinsic factors such as

423 genetic incompatibilities, potentially coupled with differences in adaptation to local

424 environments, can be present as well (Bierne *et al.*, 2011). A genome wide analysis of

425 differentiation is required to investigate whether divergence between *E. cavolini* and

426 *E. singularis*, is homogeneous along the genome (as suggested by the DILS analysis which

427 inferred a homogeneity of gene flow), or whether genomic islands of differentiation exist

428 (Peñalba *et al.*, 2024). We could then better understand to what stage of divergence the

429 *E. cavolini* / *E. singularis* split corresponds: from intra-specific polymorphism to species

430 separated by semipermeable barriers to gene flow.

431 One interesting question in this context is whether changes in selection regimes induced by

432 human activities can change the outcome of hybridization (Ålund *et al.*, 2023). For example,

433 Mediterranean octocorals are impacted by mortality events linked with climate change (Sini

434 *et al.*, 2015; Estaque *et al.*, 2023), and the impact of these events could be different for

435 hybrids and parental individuals. In scleractinian corals, interspecific hybridization has been

436 reported to enhance the survival under elevated temperature conditions (Chan *et al.*, 2018) .

437 Regarding *E. verrucosa*, the more ancient divergence corresponded to much more loci with

438 high F_{ST}. Among the list of the most highly differentiated loci, more overlap was also

439 observed for the two comparisons involving *E. verrucosa* than for the other pairwise

440 comparisons: this may indicate that few genomic areas of potential incompatibilities with

441 *E. verrucosa* are involved in the divergence between *E. cavolini* and *E. singularis*.

442

443 **Scenarios of speciations**

444

445 The scenarios of speciations inferred with DILS supported the current isolation (no gene
446 flow) of *E. verrucosa* with the two other species with high posterior probability. Conversely
447 current gene flow was strongly supported versus isolation between *E. cavolini* and
448 *E. singularis*. The posterior probabilities for ancestral migration (for *E. verrucosa* versus the
449 two other species), and secondary contact (*E. cavolini* and *E. singularis*), were lower than for
450 inferences on current gene flow. These scenarios were indeed the best ones among those
451 tested here but they might not provide the best possible representation of the evolutionary
452 history. Other models of evolution could be tested for better inferences, for example by
453 including the three species and hybrids, or gene flow from unsampled taxa (Tricou *et al.*,
454 2022). The current isolation of *E. verrucosa* from *E. cavolini* is also at odds with previous
455 results which showed the possibility of current gene flow between these two species despite
456 an important divergence (Roux *et al.*, 2016). It will be useful to explore the reasons for the
457 discrepancy between this last study and the present one, which are both based on
458 transcriptome datasets but obtained from different samples and sequencing platforms.
459 *Eunicella verrucosa* is currently widely distributed in the North Eastern Atlantic Ocean, and
460 less frequent in the Mediterranean Sea, whereas both other species are only present in the
461 Mediterranean Sea. The Atlantic / Mediterranean Sea transition does not seem to act as a
462 phylogeographic barrier for *E. verrucosa* (Macleod *et al.*, 2024). We can propose a scenario
463 where the split between *E. verrucosa* and both other species occurred in allopatry between
464 the Atlantic Ocean and the Mediterranean Sea, followed by the colonization of the
465 Mediterranean Sea by *E. verrucosa*. The generation time remains unknown for the *Eunicella*
466 species, and previous studies have shown important variation in the age at first reproduction
467 in gorgonians, from 2 to 13 years (see references in Munro, 2004). If we use a generation
468 time of two years for *Eunicella* species, with a median estimate of divergence time around
469 900 000 generations for *E. verrucosa* / *E. singularis* and 1 000 000 for *E. verrucosa* /
470 *E. cavolini*, and based on a mutation rate set at 3.10^{-9}, this would indicate a divergence at
471 least around 2 000 000 years (2 Ma). The divergence time between *E. cavolini* and
472 *E. singularis* would be 2.5 times more recent, around 800 000 years, with a median time of
473 secondary contact around 60 000 generations, corresponding to 15% of the time spent since
474 divergence. It is difficult to infer past distributions of *E. singularis* and *E. cavolini*, but one can
475 note that even if they are currently found in sympatry in different areas, their range do not
476 completely overlap. For example *E. cavolini* is nearly absent at the West of the Rhone
477 estuary on the French coast, whereas *E. singularis* is present there. The ecological range of
478 *E. singularis* and *E. cavolini* is also not completely overlapping, as *E. cavolini* can be
479 observed deeper than *E. singularis* (Gori *et al.*, 2012; Carugati *et al.*, 2022). Therefore one
480 can envision an historical separation of these two species either geographically or
481 ecologically, followed by a secondary contact where gene flow took place. In any case,

482 additional information on generation time, mutation rate and past demographic fluctuations
483 are required to be more precise on the history of these species.
484
485 **Evolution of symbiosis**
486
487 As previously discussed, we clearly demonstrated here the possibility of gene flow between
488 symbiotic (hosting Symbiodiniaceae) and non-symbiotic octocorals. Symbiodiniaceae could
489 nevertheless be involved in genetic incompatibilities with the genome of some cnidarian
490 hosts, but this would require additional analysis of symbiotic status in hybrids. The methods
491 used here did not aim at a precise quantification of Symbiodiniaceae, and one can note the
492 low levels of sequences corresponding to these symbionts, even in *E. singularis,* which may
493 be due to difficulties in extracting the RNA of the symbionts (but see Guzman *et al.*, 2018;
494 Rivera-García *et al.*, 2019). Despite these limits we observed, as expected, a higher
495 Symbiodiniaceae concentration in *E. singularis* than in *E. cavolini* and *E. verrucosa.*
496 Interestingly, the hybrids showed a lower frequency of Symbiodiniaceae than *E. singularis*,
497 and possibly than *E. cavolini*, though this last result remains to be confirmed.   In
498 *E. singularis*, the transmission of Symbiodiniaceae seems to occur both vertically, through
499 ovules, and horizontally, from the environment (Forcioli *et al.*, 2011). Both transmission
500 modes did not restore the levels of Symbiodiniaceae in the hybrids to those of *E. singularis*.
501 This suggests a breakdown of or a failure to establish symbiosis for hybrid genotypes, which
502 may impact the fitness of hybrids and consequently the possibility of introgression. The
503 *aphyta* type of *E. singularis* observed in deep conditions indicates a plasticity of symbiotic
504 status apart from hybridization. Nevertheless, here the hybrids were sampled in shallow
505 conditions (10-20 m depth) which underlines the role of hybridization in reducing the extent
506 of symbiosis. More precise estimates of Symbiodiniaceae abundance, and of physiological
507 parameters such as photosynthetic and respiration rates (Ezzat *et al.*, 2013). would help
508 understanding the role of symbionts in hybrids fitness. It would also be interesting to study if
509 the Symbiodiniaceae of the different samples belong to the same population (Pelosi *et al.*,
510 2022).
511 Our results also question the evolution and significance of octocoral / Symbiodiniaceae
512 symbiosis. In scleractinians, the transition between symbiotic and non-symbiotic states
513 happened repeatedly, but mostly in the direction of the acquisition of symbiosis, with very
514 low rates of reversal (Campoy *et al.*, 2020). This could indicate that investing in such
515 mutualistic interactions for the cnidarian would lead to increasingly relying on autotrophy for
516 energetic supply, making reversal to heterotrophy difficult. In octocorals, an evolutionary
517 versatility in symbiotic state seems possible, as in various families and genera, both
518 symbiotic and non-symbiotic species are present (Van Oppen *et al.*, 2005). In the

519 Mediterranean Sea, all octocoral species are non-symbiotic, except for *E. singularis* (but see
520 Bonacolta et al. 2024). The most parsimonious scenario here would be an acquisition of
521 symbiosis in *E. singularis* during or following its divergence from *E. cavolini*. The symbiotic
522 status of *E. singularis* nevertheless could be facultative as previously mentioned for the
523 *aphyta* type (Gori *et al.*, 2012). Additionally, experimental physiological studies have
524 demonstrated the nutritional plasticity of *E. singularis* which is able to use either heterotrophy
525 or autotrophy for its metabolism (Ezzat *et al.*, 2013). Nevertheless, in natural conditions,
526 autotrophy seems to provide an important contribution to the metabolism of *E. singularis*,
527 and the collapse of photosynthetic capacities in too warm conditions can contribute to
528 mortality events in this species (Coma *et al.*, 2015).

529 The question of symbiosis could be reversed as well: why are Symbiodiniaceae not more
530 abundant in *E. cavolini*? This species can be observed in shallow conditions (less than 10 m
531 depth) where there is enough light for photosynthesis, and in syntopy with *E. singularis*. The
532 availability of preys or particulate organic matter may provide enough energy to *E. cavolini* in
533 its habitat, but this species may have never engaged in mutualistic interaction with
534 Symbiodiniaceae. Interestingly we observed a low rate of sequences related to
535 Symbiodiniaceae in the transcriptomes of *E. cavolini* (and even lower, but not null in
536 *E. verrucosa*). This could either correspond to a signal from free living Symbiodiniaceae, or
537 to rare, transient, associations with the cnidarian. In addition, a Symbiodiniaceae OTU that is
538 common to *E. singularis* and *E. cavolini* was identified among the microeukaryotes
539 associated with the two species: this OTU is related to strains observed in symbiosis with
540 *E. singularis* and other Mediterranean cnidarians. Molecular markers also allowed to
541 evidence the presence of Symbiodiniaceae in species previously supposed to be asymbiotic,
542 as in the Mediterranean octocoral *Paramuricea clavata*, and in several Hawaiian
543 antipatharian species (Wagner *et al.*, 2011; Bonacolta *et al.*, 2024). These results, and our
544 observations in *Eunicella* species, obviously underline the dynamic nature of interactions
545 between Symbiodiniaceae and cnidarians: the establishment of symbiosis may be preceded
546 by more or less stable, and more or less mutualistic interactions. The development of
547 effective symbiosis, with stable relationships, and higher abundance of symbiont, would
548 require specific adaptation from both partners. We can see here that even if on a macro-
549 evolutionary scale the acquisition of symbiosis is much more frequent than its loss, on a
550 micro-evolutionary scale the gene flow between the *Eunicella* species considered here has
551 not led to the full development of symbiosis in *E. cavolini*.

552

553 **Conclusions and perspectives**

554

We demonstrated the lack of genetic isolation between octocorals with contrasted levels of mutualistic interaction with Symbiodiniaceae. Understanding the evolution and adaptation of these species in heterogeneous environments should then consider the possible impact of introgression. We also show that symbiosis is more flexible that previously envisioned in octocorals. For these species it will be useful to estimate the frequency and spatial extent of hybrid zones: does it correlate with particular environments with a coupling between endogenous and exogenous barriers to gene flow (Bierne *et al.*, 2011)? Characterizing the genomic landscape of introgression would help to look for the effects of introgression on adaptation or symbiosis for example. Indeed, even low levels of interspecific gene flow can have important consequences on the evolution of species (Arnold *et al.*, 1999). Finally, various cases of hybridization have been demonstrated in symbiotic anthozoans (e.g. Combosch and Vollmer, 2015; Pelosi *et al.*, 2022): it would then be interesting to study the dynamics of symbiosis in these cases, especially when different Symbiodiniaceae strains are involved.

Acknowledgements:

604 **Data availability**
605 The transcriptome raw sequences are available in Genbank under BioProject ID
606 PRJNA1037721. The RAD raw sequences are available in Genbank under BioProject ID
607 PRJNA1122331.
608 The scripts used in this study, the vcf files from RAD sequencing, and the detailed results of
609 the DILS analysis are available at https://doi.org/10.5281/zenodo.14007931
610

611 **Conflict of interest disclosure**
612 The authors declare that they have no conflict of interest in relation to the content of the
613 article
614
615

616
617 **References**
618
619

Ålund M, Cenzer M, Bierne N, *et al*. Anthropogenic Change and the Process of Speciation. *Cold Spring Harbor Perspectives in Biology* 2023;**15**:a041455. https://cshperspectives.cshlp.org/content/15/12/a041455.short

Anderson E, Thompson EA. A model-based method for identifying species hybrids using multilocus genetic data. *Genetics* 2022;**160**:1217–1229. https://academic.oup.com/genetics/article-abstract/160/3/1217/6052497

Arnold ML, Bulger MR, Burke JM, *et al*. 1999. Natural hybridization: how low can you go and still be important? *Ecology* 1999;**80**:371–381. https://esajournals.onlinelibrary.wiley.com/doi/abs/10.1890/0012-9658(1999)080[0371:NHHLCY]2.0.CO;2

Aurelle D, Pivotto ID, Malfant M, *et al*. Fuzzy species limits in Mediterranean gorgonians (Cnidaria, Octocorallia): inferences on speciation processes. *Zoologica Scripta* 2017;**46**:767–778. https://onlinelibrary.wiley.com/doi/abs/10.1111/zsc.12245

Baird NA, Etter PD, Atwood TS, *et al*. Rapid SNP Discovery and Genetic Mapping Using Sequenced RAD Markers. *PLoS ONE* 2008;**3**:e3376. https://journals.plos.org/plosone/article?id=10.1371/journal.pone.0003376

Baumgarten S, Bayer T, Aranda M, *et al*. Integrating microRNA and mRNA expression profiling in Symbiodinium microadriaticum, a dinoflagellate symbiont of reef-building corals. *BMC Genomics* 2013;**14**:704. https://link.springer.com/article/10.1186/1471-2164-14-704

Berkelmans R and van Oppen MJH. The role of zooxanthellae in the thermal tolerance of corals: a 'nugget of hope' for coral reefs in an era of climate change. *Proceedings of thex Royal Society B: Biological Sciences* 2006;**273**:2305–2312. https://royalsocietypublishing.org/doi/abs/10.1098/rspb.2006.3567

Bierne N, Borsa P, Daguin C, *et al*. Introgression patterns in the mosaic hybrid zone between Mytilus edulis and M. galloprovincialis. *Molecular Ecology* 2003;**12**:447–462. https://onlinelibrary.wiley.com/doi/abs/10.1046/j.1365-294X.2003.01730.x

Bierne N, Welch J, Loire E, *et al*. The coupling hypothesis: why genome scans may fail to map local adaptation genes. *Molecular Ecology* 2011;**20**:2044–2072. https://onlinelibrary.wiley.com/doi/abs/10.1111/j.1365-294X.2011.05080.x

Bonacolta AM, Miravall J, Gómez-Gras D, *et al*. Differential apicomplexan presence predicts thermal stress mortality in the Mediterranean coral Paramuricea clavata. *Environmental Microbiology* 2024;**26**:e16548. https://enviromicro-journals.onlinelibrary.wiley.com/doi/abs/10.1111/1462-2920.16548

Bordenstein S. Symbiosis And The Origin Of Species. In: *Insect Symbiosis*. CRC Press, 2003;283–303.

Brener-Raffalli K, Vidal-Dupiol J, Adjeroud M, *et al*. Gene expression plasticity and frontloading promote thermotolerance in *Pocillopora* corals. *Peer Community Journal* 2022;**2**. https://peercommunityjournal.org/articles/10.24072/pcjournal.79/

Brucker RM and Bordenstein SR. Speciation by symbiosis. *Trends in Ecology & Evolution* 2012;**27**:443. https://www.cell.com/trends/ecology-evolution/fulltext/S0169-5347(12)00076-6

Cabau C, Escudié F, Djari A, *et al*. Compacting and correcting Trinity and Oases RNA-Seq de novo assemblies. *PeerJ* 2017;**5**:e2988. https://peerj.com/articles/2988/

Cahill AE, Meglécz E, Chenuil A. Scientific history, biogeography, and biological traits predict presence of cryptic or overlooked species. *Biological Reviews* 2024;**99**:546-561. https://onlinelibrary.wiley.com/doi/abs/10.1111/brv.13034

Cairns SD. Deep-water corals: an overview with special reference to diversity and distribution of deep-water scleractinian corals. *Bulletin of marine Science* 2007;**81**:311–322. https://www.ingentaconnect.com/content/umrsmas/bullmar/2007/00000081/00000003/art00002

Calderón I, Garrabou J, Aurelle D. Evaluation of the utility of COI and ITS markers as tools for population genetic studies of temperate gorgonians. *Journal of Experimental Marine Biology and Ecology* 2006;**336**:184–197. https://www.sciencedirect.com/science/article/pii/S0022098106002498

Campoy AN, Addamo AM, Machordom A, *et al.* The Origin and Correlated Evolution of Symbiosis and Coloniality in Scleractinian Corals. *Frontiers in Marine Science* 2020;**7**. https://www.frontiersin.org/articles/10.3389/fmars.2020.00461/full

Carpine C, Grasshoff M. Les gorgonaires de la Méditerranée. *Bulletin de l'Institut Océanographique de Monaco* 1975*;***71**(140).

Carugati L, Moccia D, Bramanti L, *et al.* Deep-Dwelling Populations of Mediterranean Corallium rubrum and Eunicella cavolini: Distribution, Demography, and Co-Occurrence. *Biology* 2022;**11**. https://www.mdpi.com/2079-7737/11/2/333

Casado-Amezúa P, Terrón-Sigler A, Pinzón JH, *et al.* General ecological aspects of Anthozoan-Symbiodinium interactions in the Mediterranean Sea. In: Goffredo S, Dubinsky Z, (ed). The cnidaria, past, present and future: the world of medusa and her sisters. Springer, 2016;375–386. https://link.springer.com/chapter/10.1007/978-3-319-31305-4_24

Chan WY, Peplow LM, Menéndez P, Hoffmann AA & Van Oppen MJ. 2018. Interspecific hybridization may provide novel opportunities for coral reef restoration. *Frontiers in Marine Science* 5: 160. https://www.frontiersin.org/articles/10.3389/fmars.2018.00160/full

Chimienti G. 2020. Vulnerable forests of the pink sea fan Eunicella verrucosa in the Mediterranean Sea. *Diversity* 12: 176.

Coelho M, Pearson G, Boavida J, *et al.* Not out of the Mediterranean: Atlantic populations of the gorgonian Paramuricea clavata are a separate sister species under further lineage diversification. *Ecology and Evolution* 2023;**13**. https://onlinelibrary.wiley.com/doi/abs/10.1002/ece3.9740

Coma R, Llorente-Llurba E, Serrano E, *et al.* Natural heterotrophic feeding by a temperate octocoral with symbiotic zooxanthellae: a contribution to understanding the mechanisms of die-off events. *Coral Reefs* 2015;**34**:549–560. https://link.springer.com/article/10.1007/s00338-015-1281-3

Combosch DJ, Vollmer SV. Trans-Pacific RAD-Seq population genomics confirms introgressive hybridization in Eastern Pacific Pocillopora corals. *Molecular phylogenetics and evolution* 2015;**88**:154–162. https://www.sciencedirect.com/science/article/pii/S1055790315000858

Csilléry K, François O, Blum MGB. abc: an R package for approximate Bayesian computation (ABC). *Methods in Ecology and Evolution* 2012;**3**:475–479. https://besjournals.onlinelibrary.wiley.com/doi/abs/10.1111/j.2041-210X.2011.00179.x

Danecek P, Auton A, Abecasis G, *et al.* The variant call format and VCFtools. *Bioinformatics* 2011;**27**:2156–2158. https://academic.oup.com/bioinformatics/article/27/15/2156/402296

De Jode A, Le Moan A, Johannesson K,*et al.* Ten years of demographic modelling of divergence and speciation in the sea. *Evolutionary Applications* 2023;**16**:542–559. https://onlinelibrary.wiley.com/doi/abs/10.1111/eva.13428

De Queiroz K. Species Concepts and Species Delimitation. *Systematic Biology* 2007;**56**:879–886. https://academic.oup.com/sysbio/article-abstract/56/6/879/1653163

De Raad D. SNPfiltR: Interactively Filter SNP Datasets. R package version 1.0.1. https://devonderaad.github.io/SNPfiltR/, 2023

Eaton DA, Overcast I. ipyrad: Interactive assembly and analysis of RADseq datasets. *Bioinformatics* 2020;**36**:2592–2594. https://academic.oup.com/bioinformatics/article-abstract/36/8/2592/5697088

Erickson KL, Pentico A, Quattrini AM *et al.* New approaches to species delimitation and population structure of anthozoans: Two case studies of octocorals using ultraconserved elements and exons. *Molecular Ecology Resources* 2021;**21**:78–92. https://onlinelibrary.wiley.com/doi/abs/10.1111/1755-0998.13241

Estaque T, Richaume J, Bianchimani O, *et al.* Marine heatwaves on the rise: One of the strongest ever observed mass mortality event in temperate gorgonians. *Global change biology* 2023;**29**:6159-6162. https://onlinelibrary.wiley.com/doi/10.1111/gcb.16931

Ezzat L, Merle PL, Furla P, *et al.* The Response of the Mediterranean Gorgonian Eunicella singularis to Thermal Stress Is Independent of Its Nutritional Regime. *PLoS ONE* 2013;**8**:e64370. https://journals.plos.org/plosone/article?id=10.1371/journal.pone.0064370

Faria R, Johannesson K, Stankowski S. Speciation in marine environments: Diving under the surface. *Journal of Evolutionary Biology* 2021;**34**:4–15. https://academic.oup.com/jeb/article-abstract/34/1/4/7326591

Forcioli D, Merle PL, Caligara C, *et al.* Symbiont diversity is not involved in depth acclimation in the Mediterranean sea whip Eunicella singularis. *Marine Ecology Progress Series* 2011;**439**:57–71. https://www.int-res.com/abstracts/meps/v439/p57-71/

Fourt M, Goujard A. Rapport final de la campagne MEDSEACAN (Têtes des canyons méditerranéens continentaux) novembre 2008–avril 2010. *Partenariat Agence des aires marines protégées–GIS Posidonie*: 1–218. 2012. http://paleopolis.rediris.es/benthos/TaP/Rapport_Final_MEDSEACAN.pdf

Fraïsse C, Popovic I, Mazoyer C, *et al.* DILS: Demographic inferences with linked selection by using ABC. *Molecular Ecology Resources* 2021;**21**:2629–2644. https://onlinelibrary.wiley.com/doi/abs/10.1111/1755-0998.13323

Frichot E, Mathieu F, Trouillon T, *et al.* Fast and efficient estimation of individual ancestry coefficients. *Genetics* 2014;**196**:973–983. https://academic.oup.com/genetics/article/196/4/973/5935614

Frichot E, François O. LEA: an R package for landscape and ecological association studies. *Methods in Ecology and Evolution* 2015;**6**:925–929. https://besjournals.onlinelibrary.wiley.com/doi/abs/10.1111/2041-210X.12382

Furla P, Allemand D, Shick JM, *et al.* The symbiotic anthozoan: a physiological chimera between alga and animal. *Integrative and Comparative Biology* 2005;**45**:595–604. https://academic.oup.com/icb/article-abstract/45/4/595/636401

Gagnaire P, Broquet T, Aurelle D, *et al.* Using neutral, selected, and hitchhiker loci to assess connectivity of marine populations in the genomic era. *Evolutionary Applications* 2015;**8**:769–786. https://onlinelibrary.wiley.com/doi/abs/10.1111/eva.12288

Gayral P, Melo-Ferreira J, Glemin S, *et al.* Reference-free population genomics from next-generation transcriptome data and the vertebrate–invertebrate gap. *PLoS Genetics* 2013;**9**:e1003457. https://journals.plos.org/plosgenetics/article?id=10.1371/journal.pgen.1003457

Gori A, Bramanti L, López-González P, *et al.* Characterization of the zooxanthellate and azooxanthellate morphotypes of the Mediterranean gorgonian Eunicella singularis. *Marine biology* 2012;**159**:1485–1496. https://link.springer.com/article/10.1007/s00227-012-1928-3

Grasshoff,M. Die Flachwasser-Gorgonarien von Europa und Westafrika (Cnidaria, Anthozoa). *Courier Forschunginstitut Senckenberg 1992:***149**. Frankfurt a. M.

Guzman C, Shinzato C, Lu TM *et al.* Transcriptome analysis of the reef-building octocoral, Heliopora coerulea. *Scientific Reports* 2018;**8**:8397. https://www.nature.com/articles/s41598-018-26718-5

Haguenauer A, Zuberer F, Ledoux JB *et al.* Adaptive abilities of the Mediterranean red coral Corallium rubrum in a heterogeneous and changing environment: from population to functional genetics. *Journal of Experimental Marine Biology and Ecology* 2013;**449**:349–357.

Jombart T. adegenet: a R package for the multivariate analysis of genetic markers. *Bioinformatics* 2008;**24**:1403-1405. https://www.sciencedirect.com/science/article/pii/S0022098113003493

Kent WJ. BLAT—the BLAST-like alignment tool. *Genome research* 2002;**12**:656–664. https://genome.cshlp.org/content/12/4/656.short

Krueger-Hadfield S. marmap. https://www.molecularecologist.com/2015/07/03/marmap/. 2015

LaJeunesse TC, Parkinson JE, Gabrielson PW, *et al.* Systematic revision of Symbiodiniaceae highlights the antiquity and diversity of coral endosymbionts. *Current Biology* 2018;**28**:2570–2580. https://www.cell.com/current-biology/fulltext/S0960-9822(18)30907-2

LaJeunesse TC, Wiedenmann J, Casado-Amezúa P, *et al.* Revival of Philozoon Geddes for host-specialized dinoflagellates,'zooxanthellae', in animals from coastal temperate zones of northern and southern hemispheres. *European Journal of Phycology* 2022;**57**:166–180. https://www.tandfonline.com/doi/abs/10.1080/09670262.2021.1914863

Leroy T, Louvet JM, Lalanne C, *et al*. Adaptive introgression as a driver of local adaptation to climate in European white oaks. *New Phytologist* 2020;**226**:1171–1182. https://nph.onlinelibrary.wiley.com/doi/abs/10.1111/nph.16095

Lesser MP, Stat M, Gates RD. The endosymbiotic dinoflagellates (Symbiodinium sp.) of corals are parasites and mutualists. *Coral Reefs* 2013;**32**:603–611. https://link.springer.com/article/10.1007/s00338-013-1051-z

Li H, Handsaker B, Wysoker A, *et al.* The sequence alignment/map format and SAMtools. *Bioinformatics* 2009;**25**:2078–2079. https://academic.oup.com/bioinformatics/article-abstract/25/16/2078/204688

Li H, Durbin R. Fast and accurate short read alignment with Burrows–Wheeler transform. *Bioinformatics* 2009;**25**:1754–1760. https://academic.oup.com/bioinformatics/article/25/14/1754/225615

Lischer HE, Excoffier L. PGDSpider: an automated data conversion tool for connecting population genetics and genomics programs. *Bioinformatics* 2012;**28**:298–299. https://academic.oup.com/bioinformatics/article/28/2/298/198891

Lu J, Rincon N, Wood DE, *et al.* Metagenome analysis using the Kraken software suite. *Nature protocols* 2022;**17**:2815-2839. https://www.nature.com/articles/s41596-022-00738-y

Macleod KL, Jenkins TL, Witt MJ *et al.* Rare, long-distance dispersal underpins genetic connectivity in the pink sea fan, Eunicella verrucosa. *Evolutionary Applications* 2024;**17**:e13649. https://onlinelibrary.wiley.com/doi/abs/10.1111/eva.13649

Matz MV. Not-so-mutually beneficial coral symbiosis. *Current Biology* 2024:**34**(17):R798-R801.

Mayr E. Wu's genic view of speciation. *Journal of Evolutionary Biology* 2001;**14**:866–867. https://academic.oup.com/jeb/article-abstract/14/6/866/7322934

McFadden CS, Benayahu Y, Pante E, *et al.* Limitations of mitochondrial gene barcoding in Octocorallia. *Molecular Ecology Resources* 2011;**11**:19–31. https://onlinelibrary.wiley.com/doi/abs/10.1111/j.1755-0998.2010.02875.x

McFadden CS, Quattrini AM, Brugler MR, *et al.* Phylogenomics, origin, and diversification of Anthozoans (Phylum Cnidaria). *Systematic Biology* 2021;**70**:635-647. https://academic.oup.com/sysbio/article-abstract/70/4/635/6122449

Muir PR, Obura DO, Hoeksema BW, *et al.* Conclusions of low extinction risk for most species of reef-building corals are premature. *Nature Ecology & Evolution* 2022;**6**:357–358. https://www.nature.com/articles/s41559-022-01659-5

Munro L. Determining the reproductive cycle of Eunicella verrucosa. *Reef Research: ETR* 2004;**11**. https://www.marine-bio-images.com/RR_Eunicella_PDFS/Report_RR12Jul2004reproductive%20cycle%20pdf.pdf

Muthye V, Mackereth CD, Stewart JB *et al.* Large dataset of octocoral mitochondrial genomes provides new insights into mt-mutS evolution and function. *DNA repair* 2022;**110**:103273. https://www.sciencedirect.com/science/article/pii/S1568786422000027

van Oppen MJH, Medina M. Coral evolutionary responses to microbial symbioses. *Philosophical Transactions of the Royal Society B: Biological Sciences* 2020;**375**:20190591. https://royalsocietypublishing.org/doi/abs/10.1098/rstb.2019.0591

Palumbi SR. Marine speciation on a small planet. *Trends in Ecology & Evolution* 1992;**7**:114–118. https://www.sciencedirect.com/science/article/pii/016953479290144Z

Pante E, Puillandre N, Viricel A, *et al.* Species are hypotheses: avoid connectivity assessments based on pillars of sand. *Molecular Ecology* 2015a;**24**:525–544. https://onlinelibrary.wiley.com/doi/abs/10.1111/mec.13048

Pante E, Abdelkrim J, Viricel A, *et al.* Use of RAD sequencing for delimiting species. *Heredity* 2015b;**114**:450–459. https://www.nature.com/articles/hdy2014105

Pante E, Simon-Bouhet B. marmap: a package for importing, plotting and analyzing bathymetric and topographic data in R. *PLoS one* 2013;**8**:e73051. https://journals.plos.org/plosone/article?id=10.1371/journal.pone.0073051

Patro R, Duggal G, Love MI, *et al.* Salmon provides fast and bias-aware quantification of transcript expression. *Nature Methods* 2017;**14**:417–419. https://www.nature.com/articles/nmeth.4197

Pelosi JA, Bernal MA, Krabbenhoft TJ, *et al*. Fine-scale morphological, genomic, reproductive, and symbiont differences delimit the Caribbean octocorals *Plexaura homomalla* and *P. kükenthali*. *Coral Reefs*. 2022;**41**:635–653. https://link.springer.com/article/10.1007/s00338-021-02175-x

Peñalba JV, Runemark A, Meier JI, Singh P, Wogan GO, Sánchez-Guillén R, Mallet J, Rometsch SJ, Menon M, Seehausen O. The Role of Hybridization in Species Formation and Persistence. *Cold Spring Harbor perspectives in biology* 2014*;***a041445**. https://cshperspectives.cshlp.org/content/early/2024/03/01/cshperspect.a041445.short

Picard Toolkit. Broad Institute. GitHub Repository. https://broadinstitute.github.io/picard/. 2019

Porro B. Diversités génétiques chez l'holobiote Anemonia viridis: des morphotypes de l'hôte à la différenciation symbiotique. (Doctoral dissertation, COMUE Université Côte d'Azur (2015-2019). 2019. https://theses.hal.science/tel-02736573

Pudlo P, Marin JM, Estoup A, *et al.* Reliable ABC model choice via random forests. *Bioinformatics* 2016;**32**:859–866. https://academic.oup.com/bioinformatics/article-abstract/32/6/859/1744513

Quilodrán CS, Ruegg K, Sendell-Price AT, *et al.* The multiple population genetic and demographic routes to islands of genomic divergence. *Methods in Ecology and Evolution* 2020;**11**:6–21. https://besjournals.onlinelibrary.wiley.com/doi/abs/10.1111/2041-210X.13324

Readman J, Hiscock K. Eunicella verrucosa. Pink sea fan. https://www.marlin.ac.uk/species/detail/1121. 2017

Reynes L, Aurelle D, Chevalier C, *et al.* Population genomics and Lagrangian modeling shed light on dispersal events in the Mediterranean endemic Ericaria zosteroides (= Cystoseira zosteroides) (Fucales). *Frontiers in Marine Science* 2021;**8**:683528. https://www.frontiersin.org/articles/10.3389/fmars.2021.683528/full

Rivera-García L, Rivera-Vicéns RE, Veglia AJ *et al.* De novo transcriptome assembly of the digitate morphotype of Briareum asbestinum (Octocorallia: Alcyonacea) from the southwest shelf of Puerto Rico. *Marine Genomics* 2019;**47**:100676. https://www.sciencedirect.com/science/article/pii/S1874778718302393

Rosenberg E, Zilber-Rosenberg I. The hologenome concept of evolution after 10 years. *Microbiome* 2018;**6**:78. https://link.springer.com/article/10.1186/S40168-018-0457-9

Rousset F. genepop'007: a complete re-implementation of the genepop software for Windows and Linux. *Molecular Ecology Resources* 2008;**8**:103–106. https://onlinelibrary.wiley.com/doi/abs/10.1111/j.1471-8286.2007.01931.x

Rousset F, Lopez J, Belkhir K. Package 'genepop'. *R package version* 1. 2020. https://cran.r-project.org/web/packages/genepop/index.html

Roux C, Fraïsse C, Romiguier J, *et al.* Shedding Light on the Grey Zone of Speciation along a Continuum of Genomic Divergence. *PLOS Biology* 2016;**14**:e2000234. https://journals.plos.org/plosbiology/article?id=10.1371/journal.pbio.2000234

Sachs JL, Wilcox TP. A shift to parasitism in the jellyfish symbiont Symbiodinium microadriaticum. *Proceedings of the Royal Society B: Biological Sciences* 2006;**273**:425–429. https://royalsocietypublishing.org/doi/abs/10.1098/rspb.2005.3346

Sartoretto S, Francour P. Bathymetric distribution and growth rates of Eunicella verrucosa (Cnidaria: Gorgoniidae) populations along the Marseilles coast (France). *Scientia Marina* 2011;**76**:349–355. https://archimer.ifremer.fr/doc/00087/19859/

Schulz MH, Zerbino DR, Vingron M *et al.* Oases: robust de novo RNA-seq assembly across the dynamic range of expression levels. *Bioinformatics* 2012;**28**:1086–1092. https://academic.oup.com/bioinformatics/article-abstract/28/8/1086/195757

Sini M, Kipson S, Linares C, *et al.* The Yellow Gorgonian Eunicella cavolini: Demography and Disturbance Levels across the Mediterranean Sea. *PLoS ONE* 2015;**10**:e0126253. https://journals.plos.org/plosone/article?id=10.1371/journal.pone.0126253

Stanley RRE, Jeffery NW, Wringe BF, *et al.* GENEPOPEDIT: a simple and flexible tool for manipulating multilocus molecular data in R. *Molecular Ecology Resources* 2017;**17**:12–18. https://onlinelibrary.wiley.com/doi/abs/10.1111/1755-0998.12569

Tricou T, Tannier E, de Vienne DM. Ghost lineages can invalidate or even reverse findings regarding gene flow. *PLoS Biology* 2022;**20**:e3001776. https://journals.plos.org/plosbiology/article?id=10.1371/journal.pbio.3001776

Tsagkogeorga G, Cahais V, Galtier N. The population genomics of a fast evolver: high levels of diversity, functional constraint, and molecular adaptation in the tunicate Ciona intestinalis. *Genome biology and evolution* 2012;**4**:852–861. https://academic.oup.com/gbe/article-abstract/4/8/852/580636

Van Oppen M, Mieog JC, Sanchez C, *et al.* . Diversity of algal endosymbionts (zooxanthellae) in octocorals: the roles of geography and host relationships. *Molecular Ecology* 2005;**14**:2403–2417. https://onlinelibrary.wiley.com/doi/abs/10.1111/j.1365-294X.2005.02545.x

Wagner D, Pochon X, Irwin L, *et al.* Azooxanthellate? Most Hawaiian black corals contain Symbiodinium. *Proceedings of the Royal Society B: Biological Sciences* 2011;**278**:1323–1328. https://royalsocietypublishing.org/doi/abs/10.1098/rspb.2010.1681

Weir BS, Cockerham CC. Estimating F-statistics for the analysis of population structure. *Evolution* 1984;**38**:1358–1370. https://www.jstor.org/stable/2408641

Wood DE, Lu J, Langmead B. Improved metagenomic analysis with Kraken 2. *Genome Biology* 2019;**20**:257. https://link.springer.com/article/10.1186/s13059-019-1891-0

622 **Figure 1:** map of sampling sites for transcriptomes: A) general view, B) zoom on the area of
623 Marseille. The symbols correspond to different samples: EC *E. cavolini*, ES *E. singularis*, EV
624 *E. verrucosa*, HY potential hybrids. The three letters correspond to the codes of the
625 sampling. The maps have been produced with the marmap R package (Pante & Simon-
626 Bouhet, 2013) and following the tutorial of Krueger-Hadfield (2015).
627 **A)**
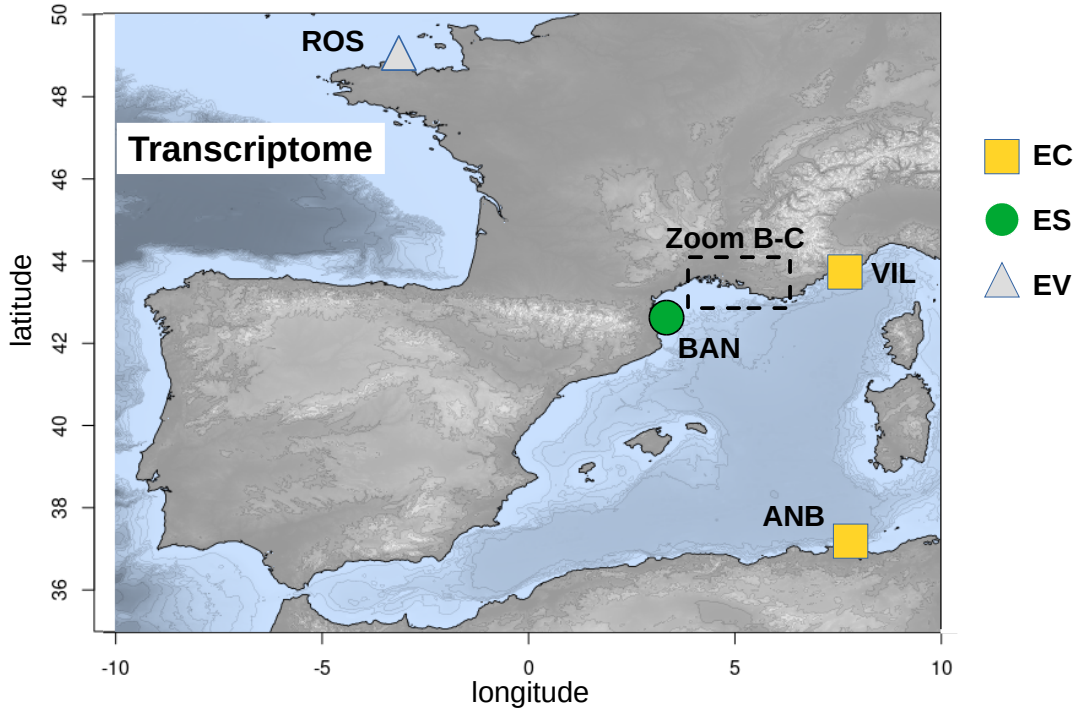
628
629 **B)**
630
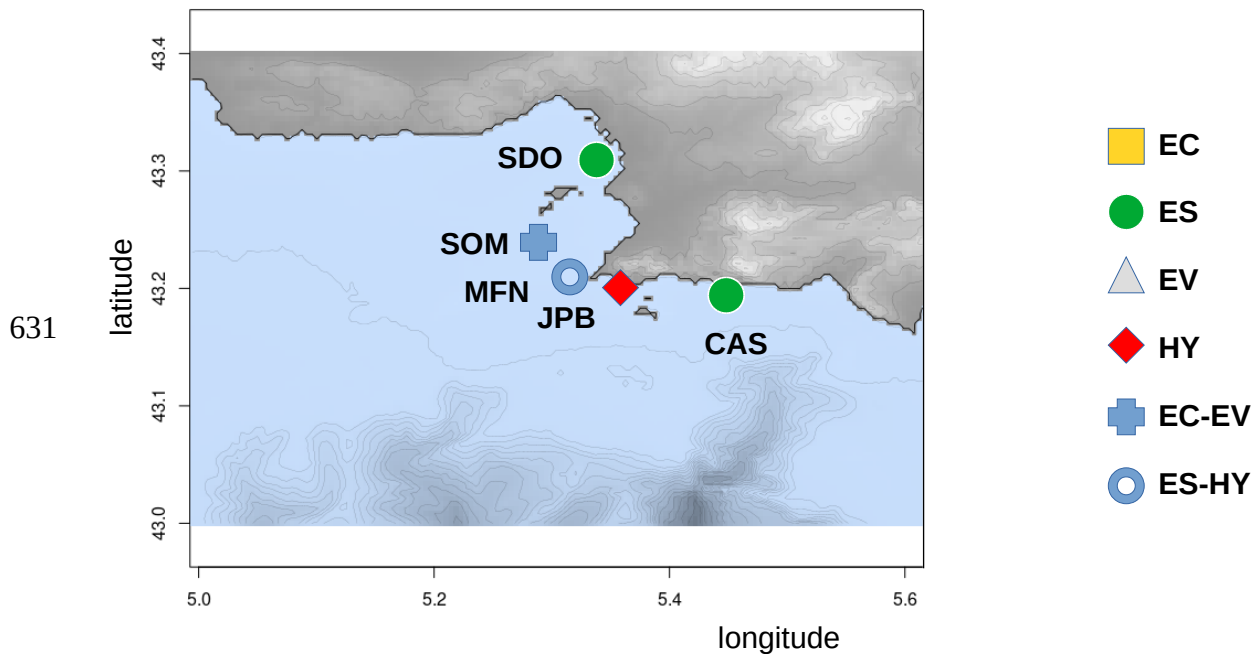
632

633 **Figure 2:** distribution of the frequency of Symbiodiniaceae sequences in the individual
634 transcriptomes according to the species based A) on the number of reads estimated with
635 Salmon, and B) on the proportion of assembled sequences (contigs) with the BLAT
636 analyses.
637
638 **A)** Read counts with Salmon; mean values per group: *E. cavolini*: 16508; hybrids: 10238;
639 *E. singularis*: 26023; *E. verrucosa*: 4285. Kruskal-Wallis test of the differences among
640 groups: chi-squared = 7.9467, df = 3, p-value = 0.047.
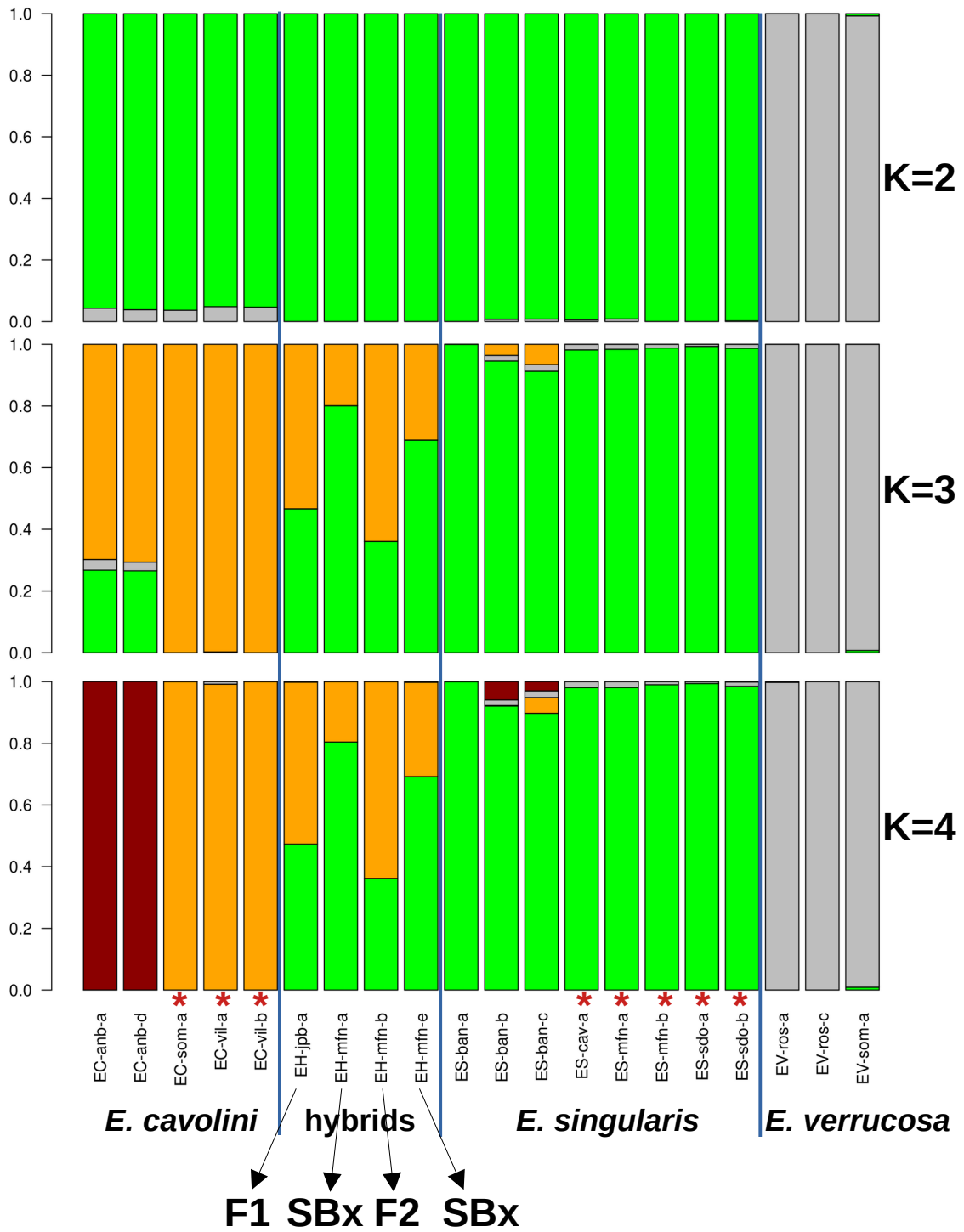

Freq. Symbiodiniaceae from salmon
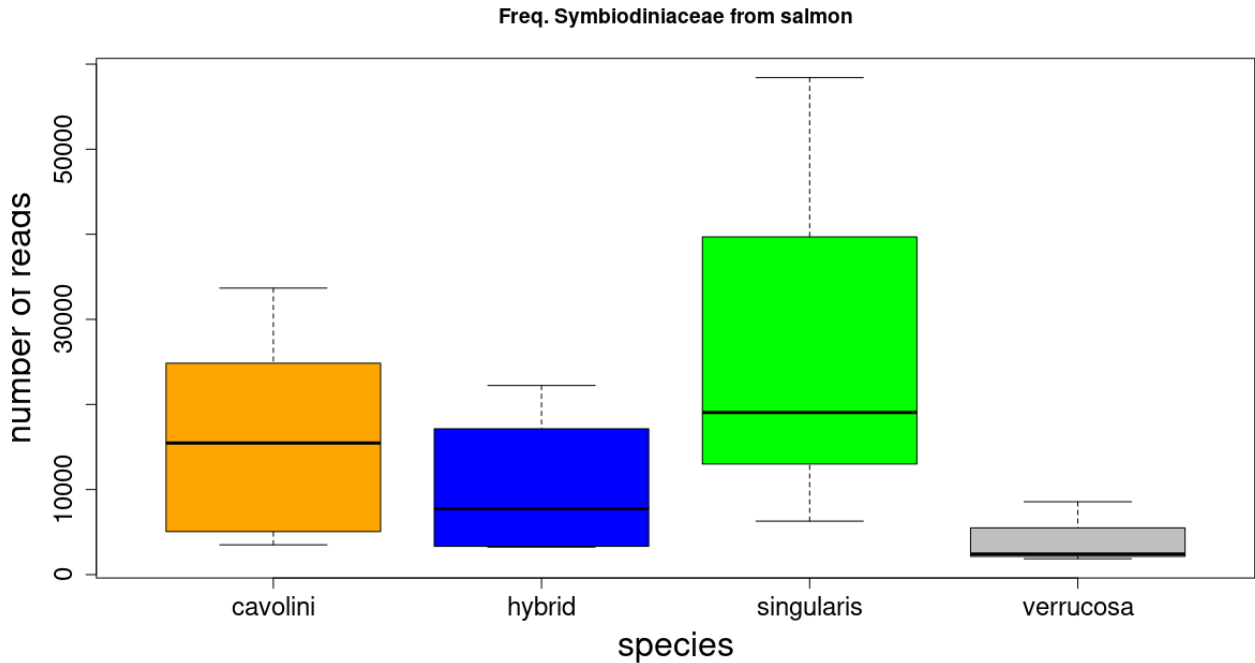
641
642
643 **B)** Assembled sequences with BLAT; mean values per group: *E. cavolini*: 0.0034; hybrids:
644 0.0029; *E. singularis*: 0.0219; *E. verrucosa*: 0.0028. Kruskal-Wallis test of the differences
645 among groups: chi-squared = 14.352, df = 3, p-value = 0.002.

Proportion Symbiodiniaceae Blat
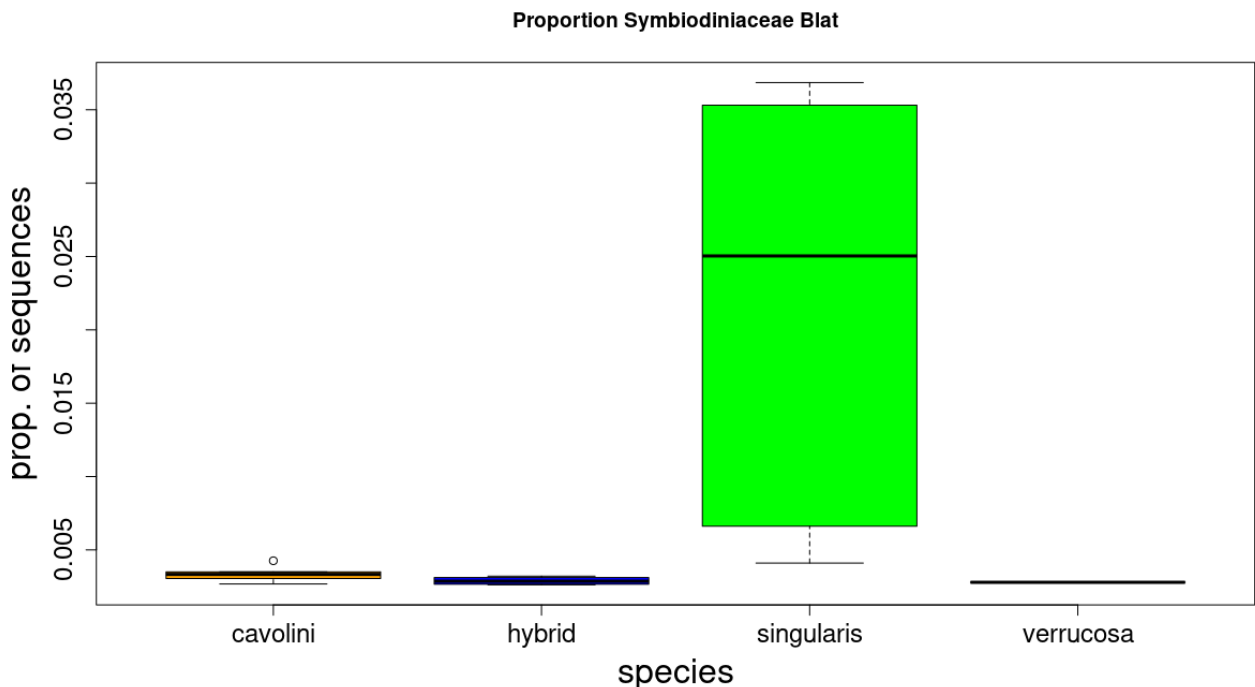
646

647 **Figure 3:** barplots of coancestry coefficients inferred with the LEA R package. The analysis
648 is based on the "polymorphic sites" transcriptome dataset. The red asterisks indicate the
649 individuals used as prior for parental status in the NewHybrids analysis. The results of the
650 NewHybrids analysis are indicated below the hybrid individuals: F1, 1st generation; F2, 2nd
651 generation; Sbx, backcross with *E. singularis*. The coancestry analysis is based on 31 369
652 SNPs, whereas the NewHybrids analysis is based on 326 SNPs showing high differentiation
653 between *E. cavolini* and *E. singularis*.
654
655

K=2

K=3

K=4

EC-anb-a EC-anb-d EC-som-a* EC-vil-a* EC-vil-b* EH-jpb-a EH-mfn-a EH-mfn-b EH-mfn-e ES-ban-a ES-ban-b ES-ban-c ES-cav-a* ES-mfn-a* ES-mfn-b* ES-sdo-a* ES-sdo-b* EV-ros-a EV-ros-c EV-som-a

E. cavolini   hybrids   *E. singularis*   *E. verrucosa*

F1 SBx F2 SBx

657
658 **Figure 4:** principal Component Analysis based on the "polymorphic SNPs" transcriptome dataset; axis 1 represents 33.2% of the variance, axis 2
659 represents 13% of the variance
660
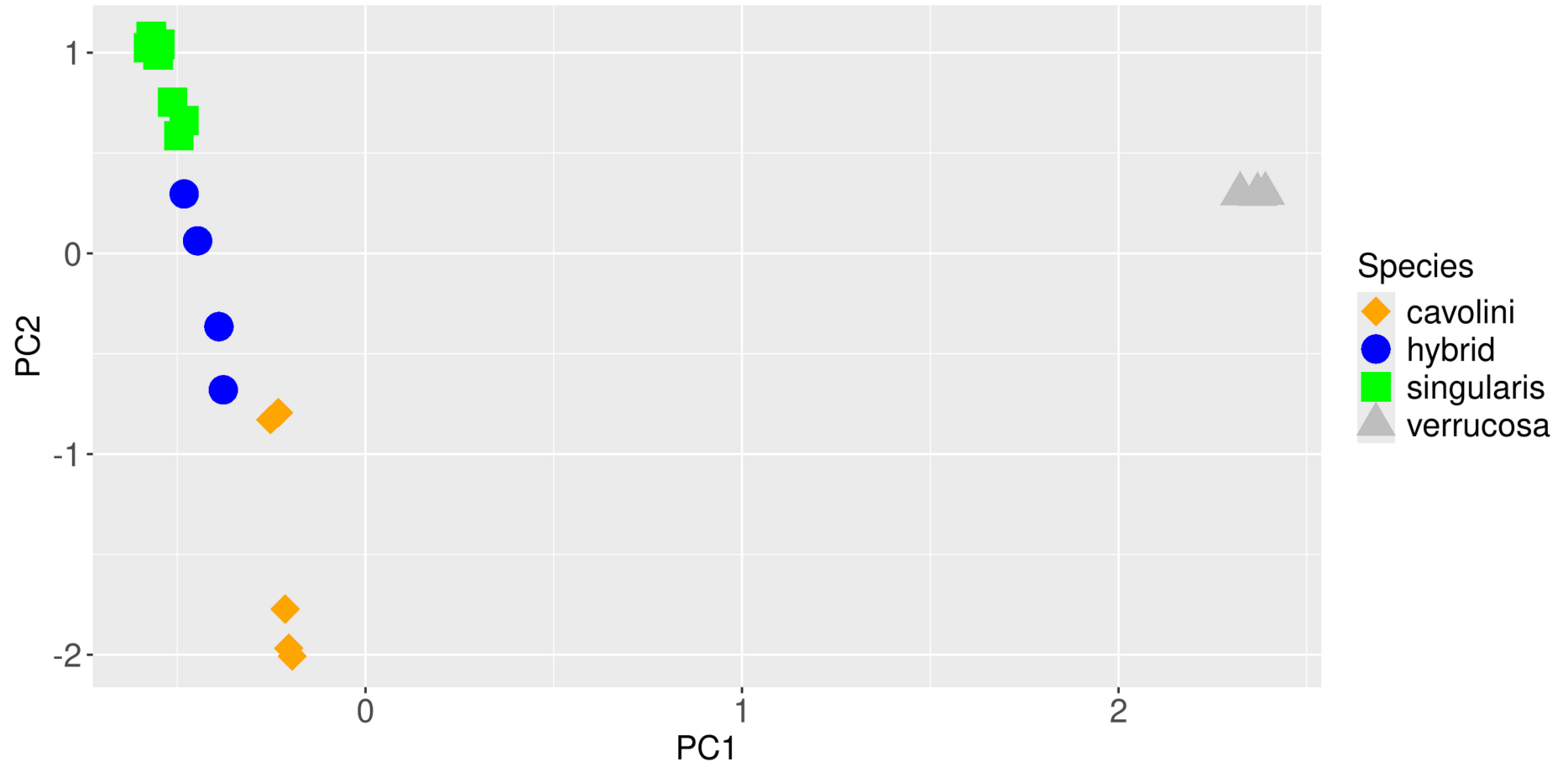
661
662
663

664 **Table 1** : inference of hybrid status with NewHybrids for transcriptome and RAD sequencing.
665 For transcriptomes, all probabilities were at 1 for the inferred status and for the ten
666 replicates. For RAD sequencing, the results are given for the four datasets (different
667 assembly strategies). If no probability is mentioned for RAD sequencing, the hybrid status
668 was supported by a probability higher than 0.999 over the ten replicates. In the other cases,
669 the numbers indicate the minimal probability threshold over the ten replicates for this status
670 (and the status was coherent over the ten replicates as well, with slight variations in
671 probability). NA indicates an individual which was removed during the filtering of SNPs
672 because of too many missing data. The lines highlighted in grey indicate the cases where
673 different status were inferred depending on the dataset. Bx-ES and Bx-EC indicate
674 backcrosses with *E. singularis* and *E. cavolini* respectively; ES indicates parental
675 *E. singularis*.

676

Individual - RAD sequencing	*de novo*	ref. *E. cavolini*	ref. *E. singularis*	ref. *E. verrucosa*
EC-X-MFNB	F2	F2	F2	F2
EC-X-MFNC	F2	NA	Bx-EC	NA
EC-X-MFND	Bx-ES	Bx-ES	Bx-ES	Bx-ES
EC-X-MFNE	Bx-EC	Bx-EC	Bx-EC	Bx-EC
EC-X-MFNF	Bx-EC	F2 > 0.95	Bx-EC > 0.92	F2
EC-X-MFNG	F2	F2	F2	F2
EC-X-MFNH	Bx-ES	Bx-ES	Bx-ES > 0.67	Bx-ES > 0.98
EC-X-MFNI	F1	F1	F1	F2
EC-X-MFNL	F1	F1 > 0.99	F1	F2
ES-X-MFNA	Bx-ES	Bx-ES	Bx-ES	Bx-ES
ES-X-MFNJ	F2	F2 > 0.96	F2	F2
ES-X-MFNK	ES	ES	ES	ES
Individual - transcriptome				
EH-JPB-a	F1			
EH-MFN-a	Bx-ES			
EH-MFN-b	F2			
EH-MFN-e	Bx-ES			

677

678 **Table 2:** results of demographic inferences with DILS with transcriptome data. The columns indicate the species comparison, the model choice for
679 population size (constant vs. variable), and the results of inferences: current (on-going) gene flow (migration vs isolation); if current migration is
680 inferred DILS compares isolation / migration (IM) with secondary contact (SC); if no current migration is inferred, the comparison is between strict
681 isolation (SI) and ancestral migration (AM); the last columns give the results of the tests of homogeneity or heterogeneity among loci for inferences in
682 effective size (N-homo vs N-hetero), and gene flow (M-homo vs M-hetero). The probability of each scenario is given in the same case. Homogeneity
683 and heterogeneity indicate no variation or variation among loci respectively.
684

Comparison	Population size	Current gene flow	IM / SC	SI / AM	N-hetero / N-homo	M-hetero / M-homo
cavolini / singularis	constant	Migration; 0.87	SC; 0.79	-	N-hetero; 0.99	M-homo; 0.82
cavolini / singularis	variable	Migration; 0.88	SC; 0.77	-	N-hetero; 1	M-homo; 0.87
cavolini / verrucosa	constant	Isolation; 0.90	-	AM; 0.65	N-hetero; 1	-
cavolini / verrucosa	variable	Isolation; 0.89	-	AM; 0.69	N-hetero; 1	-
singularis / verrucosa	constant	Isolation; 0.87	-	AM; 0.61	N-hetero; 1	-
singularis / verrucosa	variable	Isolation; 0.87	-	AM; 0.61	N-hetero; 1	-

685

Symbiotic status does not preclude hybridisation in Mediterranean octocorals

Supplementary Material S1

Didier Aurelle[1,2*], Anne Haguenauer[3], Marc Bally[1], Frédéric Zuberer[4], Jean-Baptiste Ledoux[5], Stéphane Sartoretto[6], Lamya Chaoui[7], Hichem Kara[7], Sarah Samadi[2], Pierre Pontarotti[8,9,10]

[1] Aix Marseille Univ, Université de Toulon, CNRS, IRD, MIO, Marseille, France

[2] Institut Systématique Evolution Biodiversité (ISYEB), Muséum national d'Histoire naturelle, CNRS, Sorbonne Université, EPHE, Université des Antilles, CP 26, 75005 Paris, France.

[3] CNRS - Délégation Provence et corse, Marseille, France

[4] Aix Marseille Univ, CNRS, IRD, INRAE, OSU Inst. PYTHEAS, Marseille, France

[5] CIIMAR/CIMAR, Centro Interdisciplinar de Investigação Marinha e Ambiental, Universidade do Porto, Porto, Portugal.

[6] Ifremer, LITTORAL, 83500 La Seyne-sur-Mer, France

[7] Laboratoire Bioressources marines. Université d'Annaba Badji Mokhtar, Annaba - Algérie.

[8] Aix Marseille Univ, MEPHI, Marseille, France.

[9] IHU Méditerranée Infection, Marseille, France.

[10] CNRS SNC5039

*Corresponding author

Correspondence: didier.aurelle@univ-amu.fr

Table S1 : samples used for RAD sequencing, with putative species on the basis of field identications. All sampling sites are in the area of Marseille (see Figure 1).

Sample	morphologial identification	sampling year	site	depth (m)	raw reads
ECESC37	*E. cavolini*	2020	Escu	10	4588103
ECESC38	*E. cavolini*	2020	Escu	10	7379895
ECESC39	*E. cavolini*	2020	Escu	10	7749308
ECMEL37	*E. cavolini*	2020	Mélette	20	10448058
ECPLD22	*E. cavolini*	2020	Veyron	40	9621675
ECPLD23	*E. cavolini*	2020	Veyron	40	9266239
ECPLD24	*E. cavolini*	2020	Veyron	40	4517126
ECPLD25	*E. cavolini*	2020	Veyron	40	4363166
ECPLD26	*E. cavolini*	2020	Veyron	40	5409613
ECPLD38	*E. cavolini*	2020	Veyron	40	8258381
ECPLD39	*E. cavolini*	2020	Veyron	40	5241648
ECRID13	*E. cavolini*	2020	Riou	40	5146046
ECRID14	*E. cavolini*	2020	Riou	40	4743650
ECRID15	*E. cavolini*	2020	Riou	40	4639611
ECRID16	*E. cavolini*	2020	Riou	40	11001580
ECRID17	*E. cavolini*	2020	Riou	40	10657450
ECRID19	*E. cavolini*	2020	Riou	40	6801196
ECRID20	*E. cavolini*	2020	Riou	40	4546053
ECRID21	*E. cavolini*	2020	Riou	40	6800451
ECRID22	*E. cavolini*	2020	Riou	40	5310390
ECRID23	*E. cavolini*	2020	Riou	40	4702724
ECRID25	*E. cavolini*	2020	Riou	40	5472492
ECRID27	*E. cavolini*	2020	Riou	40	8302669
ECRID28	*E. cavolini*	2020	Riou	40	9097420
ECRID29	*E. cavolini*	2020	Riou	40	8163462
ESFRO10	*E. singularis*	2022	Fromages	10-25	9983228
ESFRO11	*E. singularis*	2022	Fromages	10-25	9752609
ESFRO12	*E. singularis*	2022	Fromages	10-25	13963735
ESFRO13	*E. singularis*	2022	Fromages	10-25	7473750
ESFRO14	*E. singularis*	2022	Fromages	10-25	11379910
ESFRO15	*E. singularis*	2022	Fromages	10-25	7291156
ESFRO2	*E. singularis*	2022	Fromages	10-25	5024054
ESFRO3	*E. singularis*	2022	Fromages	10-25	6235592
ESFRO5	*E. singularis*	2022	Fromages	10-25	3539506
ESFRO6	*E. singularis*	2022	Fromages	10-25	6217585
ESFRO7	*E. singularis*	2022	Fromages	10-25	12405704
ESFRO8	*E. singularis*	2022	Fromages	10-25	14113042
ESFRO9	*E. singularis*	2022	Fromages	10-25	13734698

ESSFI1	*E. singularis*	2013	Figuier	15	3885117
ESSFI10	*E. singularis*	2013	Figuier	15	4886425
ESSFI2	*E. singularis*	2013	Figuier	15	9360315
ESSFI3	*E. singularis*	2013	Figuier	15	12083132
ESSFI4	*E. singularis*	2013	Figuier	15	5542586
ESSFI5	*E. singularis*	2013	Figuier	15	5957124
ESSFI6	*E. singularis*	2013	Figuier	15	5030751
ESSFI7	*E. singularis*	2013	Figuier	15	7657655
ESSFI8	*E. singularis*	2013	Figuier	15	4283226
ESSFI9	*E. singularis*	2013	Figuier	15	5367231
EVCSO2	*E. verrucosa*	2022	Fromages	10-25	3794532
EVCSO4	*E. verrucosa*	2022	Fromages	10-25	6731471
EVFRO1	*E. verrucosa*	2022	Fromages	10-25	7811130
EVFRO2	*E. verrucosa*	2022	Fromages	10-25	4631737
EVFRO3	*E. verrucosa*	2022	Fromages	10-25	4507318
EVFRO4	*E. verrucosa*	2022	Fromages	10-25	3661582
EVFRO5	*E. verrucosa*	2022	Fromages	10-25	5269993
EC-X-MFNB	intermediate	2013	Maïre	10	5903675
EC-X-MFNC	intermediate	2013	Maïre	10	3478362
EC-X-MFND	intermediate	2013	Maïre	10	5023674
EC-X-MFNE	intermediate	2013	Maïre	10	5102971
EC-X-MFNF	intermediate	2013	Maïre	10	3427364
EC-X-MFNG	intermediate	2013	Maïre	10	4594893
EC-X-MFNH	intermediate	2013	Maïre	10	9326619
EC-X-MFNI	intermediate	2013	Maïre	10	6228674
EC-X-MFNL	intermediate	2013	Maïre	10	6013320
ES-X-MFNA	intermediate	2013	Maïre	10	5686156
ES-X-MFNJ	intermediate	2013	Maïre	10	5972257
ES-X-MFNK	intermediate	2013	Maïre	10	5383938

Table S2 : list of samples (all sampled in 2016) and statistics of assembled transcriptomes for individual transcriptomes and meta-transcriptomes. The intermediate samples correspond to individuals with intermediate morphology, suspected to be hybrids before genetic analyses. For Annaba and Villefranche sur Mer, we indicate a range depth, as the precise sampling depth had not been recorded. The assembly is based on paired-ends sequencing (2 x 75 bp) and the number of raw sequences corresponds to the number of pairs. Contigs indicates the number of contigs for each assembly, with the corresponding N50 and L50. The Lg columns corresponds to the contigs length in bp, with the sum, minimum, mean, median and maximum of Lg. The last two lanes refer to the meta-transcriptome obtained from all individual transcriptomes with or without potential Symbiodiniaceae sequences. See main text for details.

morphologial identification	sample	site	depth	raw sequences	contigs	N50	L50	Lg sum	Lg min	Lg mean	Lg median	Lg max
E. cavolini	e-cavol-anb-a	Annaba, Algeria	20-30	21432997	33627	1978	7240	46041698	201	1369.19	1023	13533
E. cavolini	e-cavol-anb-d	Annaba, Algeria	20-30	20070761	33624	2002	7025	46288676	201	1376.66	1004	24422
E. cavolini	e-cavol-som-a	Marseille, France	58	22986734	43541	1757	8987	52113269	201	1196.88	840	24228
E. cavolini	e-cavol-vil-a	Villefranche sur Mer, France	20-40	31846763	36908	2056	7687	51709228	201	1401.03	1018	18381
E. cavolini	e-cavol-vil-b	Villefranche sur Mer, France	20-40	28751407	34961	2044	7470	48971519	201	1400.75	1040	19504
intermediate	e-hybri-jpb-a	Marseille, France	25	34392918	39407	2031	8098	54290945	201	1377.7	998	25557
intermediate	e-hybri-mfn-a	Marseille, France	10	44256795	40762	2081	8451	57794280	201	1417.85	1039	25573
intermediate	e-hybri-mfn-b	Marseille, France	10	34705411	39672	2046	8040	54738734	201	1379.78	981.5	16650
intermediate	e-hybri-mfn-e	Marseille, France	10	36536647	39532	2038	8090	54685655	201	1383.33	995.5	25578
E. singularis	e-singu-ban-a	Banyuls, France	10	44325669	45364	1919	9379	58576839	201	1291.26	928	28882
E. singularis	e-singu-ban-b	Banyuls, France	10	33184944	38095	1930	8114	50868966	201	1335.32	987	20211
E. singularis	e-singu-ban-c	Banyuls, France	10	46271612	43821	2023	9132	60512898	201	1380.91	1007	21714
E. singularis	e-singu-cav-a	Marseille, France	25	48947180	51120	1967	10031	65261049	201	1276.62	868	22527
E. singularis	e-singu-mfn-a	Marseille, France	10	52588076	70114	1761	13336	79649263	201	1136	739	16808
E. singularis	e-singu-mfn-b	Marseille, France	10	43713977	55035	1894	10583	67120524	201	1219.6	808	21143
E. singularis	e-singu-sdo-a	Marseille, France	30	37444166	55928	1741	10464	62326140	201	1114.4	715	16387
E. singularis	e-singu-sdo-b	Marseille, France	30	39266148	72419	1652	13837	78950323	201	1090.19	715	24245
E. verrucosa	e-verru-ros-a	Roscoff, France	20	19398629	31195	1936	6630	41727111	201	1337.62	981	16974
E. verrucosa	e-verru-ros-c	Roscoff, France	20	20495748	31526	1968	6729	42779660	201	1356.96	1005	16663
E. verrucosa	e-verru-som-a	Marseille, France	58	23332185	33133	2005	6944	45531674	201	1374.21	1005	25577

Meta transcriptome				number of contigs	retained contigs	N50	L50	Lg sum	Lg min	Lg mean	Lg median	Lg max
meta				891354	68386	2144	14309	102621319	201	1500,62	1098	28882
meta no Symb				300085	59697	1975	12316	80903965	201	1355,24	967	25577

Table S3: list of mitochondrial MutS sequences used for the phylogenetic reconstruction with the corresponding Genbank accession numbers. The location and voucher code are indicated when available.

Accession number	Genus	species	location	voucher
KP036906	*Complexum*	*monodi*	*Congo*	*CSM-SEN3*
NC_035666	*Eunicella*	*albicans*	-	*SNSB-BSPG 2015 XXXI GW1815*
JQ397290	*Eunicella*	*cavolini*	*Isola d'Elba*	-
JQ397291	*Eunicella*	*cavolini*	*Isola d'Elba*	-
JQ397292	*Eunicella*	*cavolini*	*Isola d'Elba*	-
NC_035667	*Eunicella*	*cavolinii*	-	*SNSB-BSPG 2015 XXXI GW4597*
KX051577	*Eunicella*	*racemosa*	*Atlantic - Morocco*	*BEIM-26*
JQ397293	*Eunicella*	*singularis*	*Cap de Creus*	-
JQ397294	*Eunicella*	*singularis*	*Cap de Creus*	-
KX051571	*Eunicella*	*singularis*	*Cap de Creus*	*BEIM-11*
KX051572	*Eunicella*	*singularis*	*Cap de Creus*	*BEIM-13*
JQ397307	*Eunicella*	*sp.*	-	-
JQ397308	*Eunicella*	*sp.*	-	-
JQ397311	*Eunicella*	*sp.*	-	-
JX203795	*Eunicella*	*tricoronata*	-	*RMNH Coel.40814*
NC_062012	*Eunicella*	*tricoronata*	-	-
JQ397300	*Eunicella*	*verrucosa*	*Tarragona*	-
JQ397302	*Eunicella*	*verrucosa*	*Tarragona*	-
JQ397305	*Eunicella*	*verrucosa*	*Tarragona*	-
JQ397306	*Eunicella*	*verrucosa*	*Tarragona*	-
NC_073494	*Eunicella*	*verrucosa*	*United Kingdom: England, Lyme Bay, East, Tennants Reef*	-
KX904973	*Swiftia*	*pacifica*	-	-
KX905018	*Swiftia*	*simplex*	-	-

Table S4 : summary of the different datasets; for transcriptomes, the first four datasets include variable and non variable sites (all sites), while the "polymorphic sites" and the "1% SNPs" datasets only consider SNPs, i.e. variable sites. For the "all" datasets we indicate the number of contigs and the number of sites retained from reads2snp. See main text for details

dataset	samples	sites / assembly	number of individuals	number of contigs / SNPs	analyses
RAD sequencing					
RAD_denovo	all	all, *de novo* assembly	67	16362 SNPs	F_{ST}, LEA
RAD_EC	all	all, assembly on *E. cavolini* genome	65	12952 SNPs	F_{ST}, LEA
RAD_ES	all	all, assembly on *E. singularis* genome	67	13342 SNPs	F_{ST}, LEA
RAD_EV	all	all, assembly on *E. verrucosa* genome	65	29061 SNPs	F_{ST}, LEA, PCA
RAD_denovo 1%	without *verrucosa*	1 % highest F_{ST} *cavolini* / *singularis*	67	163 SNPs	NewHybrids
RAD_EC 1%	without *verrucosa*	1 % highest F_{ST} *cavolini* / *singularis*	65	130 SNPs	NewHybrids
RAD_ES 1%	without *verrucosa*	1 % highest F_{ST} *cavolini* / *singularis*	67	133 SNPs	NewHybrids
RAD_EV 1%	without *verrucosa*	1 % highest F_{ST} *cavolini* / *singularis*	65	290 SNPs	NewHybrids
Transcriptomes					
all sites	all	all from reads2snp	20	61500 contigs / 101516577 sites	build SNPs datasets

all-CS	*cavolini / singularis*	all from reads2snp	20	61947 contigs / 101515803 sites	speciation scenarios with DILS
all-CV	*cavolini / verrucosa*	all from reads2snp	20	59702 contigs / 100704015 sites	speciation scenarios with DILS
all-SV	*singularis / verrucosa*	all from reads2snp	20	61373 contigs / 101444729 sites	speciation scenarios with DILS
polymorphic sites	all	polymorphic sites ; no missing data	20	31369 SNPs	F_{ST}, LEA, PCA
1 % SNPs	without *verrucosa*	polymorphic sites ; no missing data ; 1 % highest F_{ST} *cavolini / singularis*	20	326 SNPs	NewHybrids

Table S5: parameters used in the DILS analyses: Max_NA : maximum proportion of missing data ; Lmin : minimum sequence length per gene ; nMin : minimum number of sequences per gene and per species ; jSFS : use of joint Site Frequency Spectrum as an additional set of summary statistics ; constant / variable : consider constant or variable population size ; minimum and maximum values for the following priors : Tsplit : time of split, Ne : population size, M : migration rate. All other priors were kept at default values. For all analyses we used the option for coding regions, we didn't use any outgroup, we used the bimodal model for barriers, and the "normal" computation mode. The last column indicates the code used to describe the corresponding analysis in the text. The ranges of prior were chosen after preliminary analyses where we analysed the goodness of fit of the data to the models and priors. We used a mutation rate of 3.10^{-9}.

dataset	max_NA	Lmin	nMin	jSFS	Tsplit	Ne	M
all-CS	0.1	30	10	yes	100 – 2 000 000	100 – 2 000 000	0-30
all-CV	0.1	30	6	yes	100 – 2 000 000	100 – 2 000 000	0-30
all-SV	0.1	30	6	yes	100 – 2 000 000	100 – 2 000 000	0-30

Table S6: frequency of Symbiodiniaceae sequences in the individual transcriptomes on the basis i) of the proportion of raw reads mapped on the Symbiodiniaceae transcriptome, and ii) on the proportion of contigs in individual transcriptomes following the BLAT analysis. "meta" indicate the meta-transcriptome assembly based on all samples. See Table S2 for the codes of samples.

Sample	Species	Raw reads	Transcriptome
e-cavol-anb-a	*E. cavolini*	0.0171	0.00305
e-cavol-anb-d	*E. cavolini*	0.0087	0.00268
e-cavol-som-a	*E. cavolini*	0.0087	0.00426
e-cavol-vil-a	*E. cavolini*	0.0184	0.00350
e-cavol-vil-b	*E. cavolini*	0.0255	0.00333
e-hybri-jpb-a	hybrid	0.0123	0.00262
e-hybri-mfn-a	hybrid	0.0076	0.00321
e-hybri-mfn-b	hybrid	0.0079	0.00270
e-hybri-mfn-e	hybrid	0.0162	0.00302
e-singu-ban-a	*E. singularis*	0.0192	0.00675
e-singu-ban-b	*E. singularis*	0.0140	0.00410
e-singu-ban-c	*E. singularis*	0.0080	0.00647
e-singu-cav-a	*E. singularis*	0.0261	0.02263
e-singu-mfn-a	*E. singularis*	0.0233	0.03419
e-singu-mfn-b	*E. singularis*	0.0129	0.02745
e-singu-sdo-a	*E. singularis*	0.0158	0.03644
e-singu-sdo-b	*E. singularis*	0.0207	0.03686
e-verru-ros-a	*E. verrucosa*	0.0075	0.00276
e-verru-ros-c	*E. verrucosa*	0.0082	0.00282
e-verru-som-a	*E. verrucosa*	0.0098	0.00279
meta			0.01393

Table S7: p-values of the Pairwise-Wilcoxon test on the frequency of Symbiodiniaceae. A) on the basis of read counts with Salmon; B) on the proportion of assembled sequences with the BLAT analysis

A)

	E. cavolini	hybrids	*E. singularis*
hybrids	0.69		
E. singularis	0.69	0.36	
E. verrucosa	0.57	0.69	0.15

B)

	E. cavolini	hybrids	*E. singularis*
hybrids	0.571		
E. singularis	0.019	0.020	
E. verrucosa	0.571	1	0.048

Table S8: RAD sequencing data; pairwise F_{ST} estimated from all SNPs after filtering, for the four assembly strategies

de novo assembly

	E. cavolini	hybrids	E. singularis	E. verrucosa
E. cavolini	-			
hybrids	0.156	-		
E. singularis	0.380	0.122	-	
E. verrucosa	0.587	0.574	0.658	-

assembly on the genome of *E. cavolini*

	E. cavolini	hybrids	E. singularis	E. verrucosa
E. cavolini	-			
hybrids	0.155	-		
E. singularis	0.361	0.113	-	
E. verrucosa	0.563	0.553	0.630	-

assembly on the genome of *E. singularis*

	E. cavolini	hybrids	E. singularis	E. verrucosa
E. cavolini	-			
hybrids	0.141	-		
E. singularis	0.352	0.114	-	
E. verrucosa	0.563	0.554	0.634	-

assembly on the genome of *E. verrucosa*

	E. cavolini	hybrids	*E. singularis*	*E. verrucosa*
E. cavolini	-			
hybrids	0.126	-		
E. singularis	0.294	0.093	-	
E. verrucosa	0.514	0.515	0.568	-

Table S9: transcriptome data; above diagonal: average net divergence estimated from DILS for the "all" pairwise datasets (the hybrids were not included in the DILS analysis); below diagonal pairwise F_{ST} estimated from variable sites only ("polymorphic SNPs" dataset; see main text and Table S3 for details)

	E. cavolini	hybrids	*E. singularis*	*E. verrucosa*
E. cavolini	-	-	0.0018	0.0067
hybrids	0.069	-	-	-
E. singularis	0.207	0.073	-	0.0070
E. verrucosa	0.432	0.456	0.529	-

Table S9: estimated parameters for the different evolutionary scenarios for the three pairwise comparisons. We present here the results of estimations for the optimized posterior with the random forests approach implemented in DILS. For each parameter we present the highest posterior density (HPD), with the median, and the lower and higher 2.5 % limits. Models : SC : secondary contact ; AM : ancestral migration. Parameters : N : effective size ; founders$_X$: number of founder individuals in species X ; T$_{split}$: time of split at which the ancestral population subdivides in two populations ; T$_{SC}$: time of secondary contact ; T$_{AM}$: time of the end of gene flow for ancestral migration ; T$_{dem\_X}$: time of demographic event for species X ; M$_{XY}$: introgression rate from Y to X . For all parameters, the subscripts indicate the species : A for ancestral, C for *E. cavolini*, S for *E. singularis,* and V for *E. verrucosa*. Times are given in generations, migration in numbers of migrants per generation.

A) comparison *E. cavolini / E. singularis*

	HPD 0.025	HPD median	HPD 0.0975
constant size, SC			
N_C	545985	633894	733842
N_S	168290	192199	225073
N_A	537403	581831	632310
T_{split}	336413	403273	476196
T_{SC}	51536	62039	71760
M_{CS}	12	15	17
M_{SC}	12	15	18
variable size, SC			
N_C	531986	665965	875780
N_S	185826	222258	276889
N_A	515018	578861	640504
$founders_C$	0	1	1
$founders_S$	0	1	1
T_{dem_C}	250520	339056	418963
$T_{demS\_}$	245400	350132	454320
T_{split}	330907	434060	542765
T_{SC}	40560	57552	75405
M_{CS}	14	19	24
M_{SC}	8	12	16

B) comparison *E. cavolini / E. verrucosa*

	HPD 0.025	HPD median	HPD 0.0975
constant size, AM			
N_C	630969	744556	875220
N_V	648850	755298	920095
N_A	698501	784512	879664
T_{split}	909392	1054488	1225792
T_{AM}	840920	991118	1147073
M_{CV}	4	6	7
M_{VC}	9	12	14
variable size, AM			
N_C	777526	1099410	1694348
N_V	871210	1230360	1803231
N_A	692366	793880	930000
$founders_C$	0	1	1
$founders_V$	0	0	1
T_{dem_C}	237960	369260	496633
T_{dem_V}	335620	509096	679348
T_{split}	819714	1051517	1367074
T_{AM}	782210	930590	1104120
M_{CV}	7	12	16
M_{VC}	11	22	31

C) comparison *E. singularis / E. verrucosa*

	HPD 0.025	HPD median	HPD 0.0975
constant size, AM			
N_S	263390	298162	336536
N_V	490519	592796	715930
N_A	632004	708517	790246
T_{split}	741840	899098	1091610
T_{AM}	698891	811827	934655
M_{SV}	10	14	17
M_{VS}	21	27	33
variable size, AM			
N_S	281023	386388	494606
N_V	856542	1165039	1566087
N_A	592428	697054	797828
$founders_C$	0	0	0
$founders_V$	0	0	1
T_{dem_S}	166517	273546	374076
T_{dem_V}	226988	360174	493360
T_{split}	713634	926756	1207281
T_{AM}	454059	659458	858558
M_{SV}	3	4	6
M_{VS}	1	1	2

Figure S1: examples of morphological diversity in *Eunicella* species in the area of Marseille. See Carpine and Grasshoff (1975) for details.
A) example of typical *E. cavolini* colonies (in the foreground): color yellow - orange, calyces relatively low.
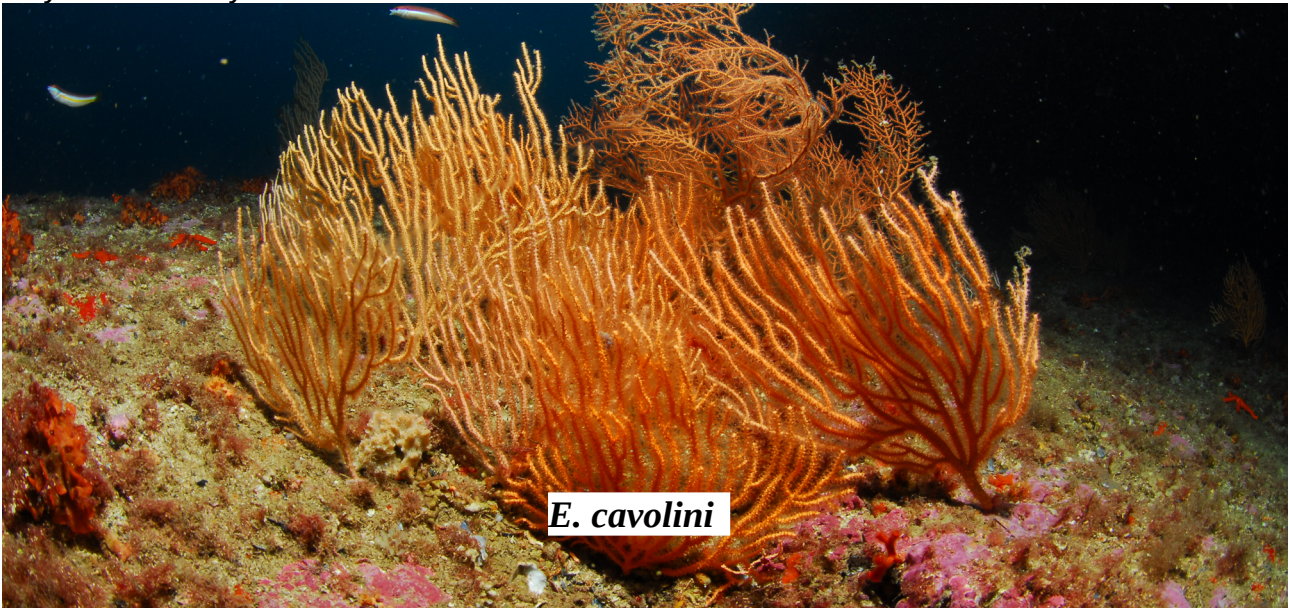
B) example of a typical *E. singularis*: color white, long terminal branches, calyces not projecting.
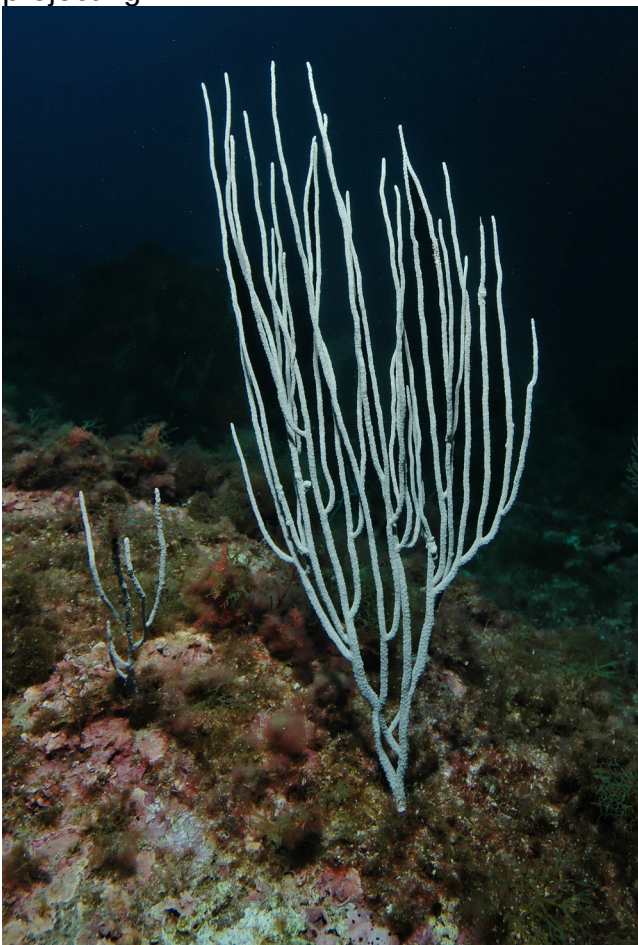
C) example of a typical *E. verrucosa*: color white or pale pink, calyces high.
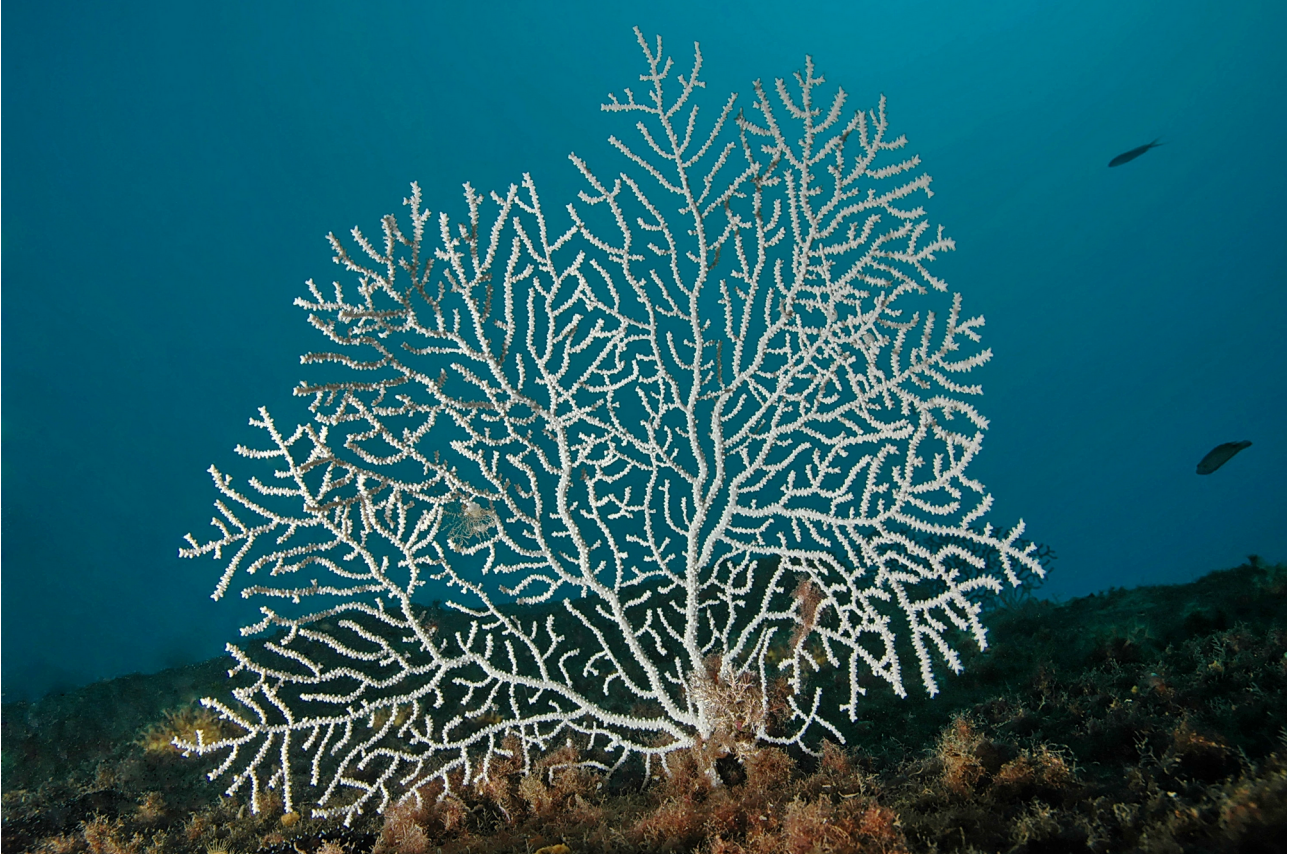
D) sampling with the presence of *E. cavolini* (EC), *E. singularis* (ES) and a potential hybrid (EH).
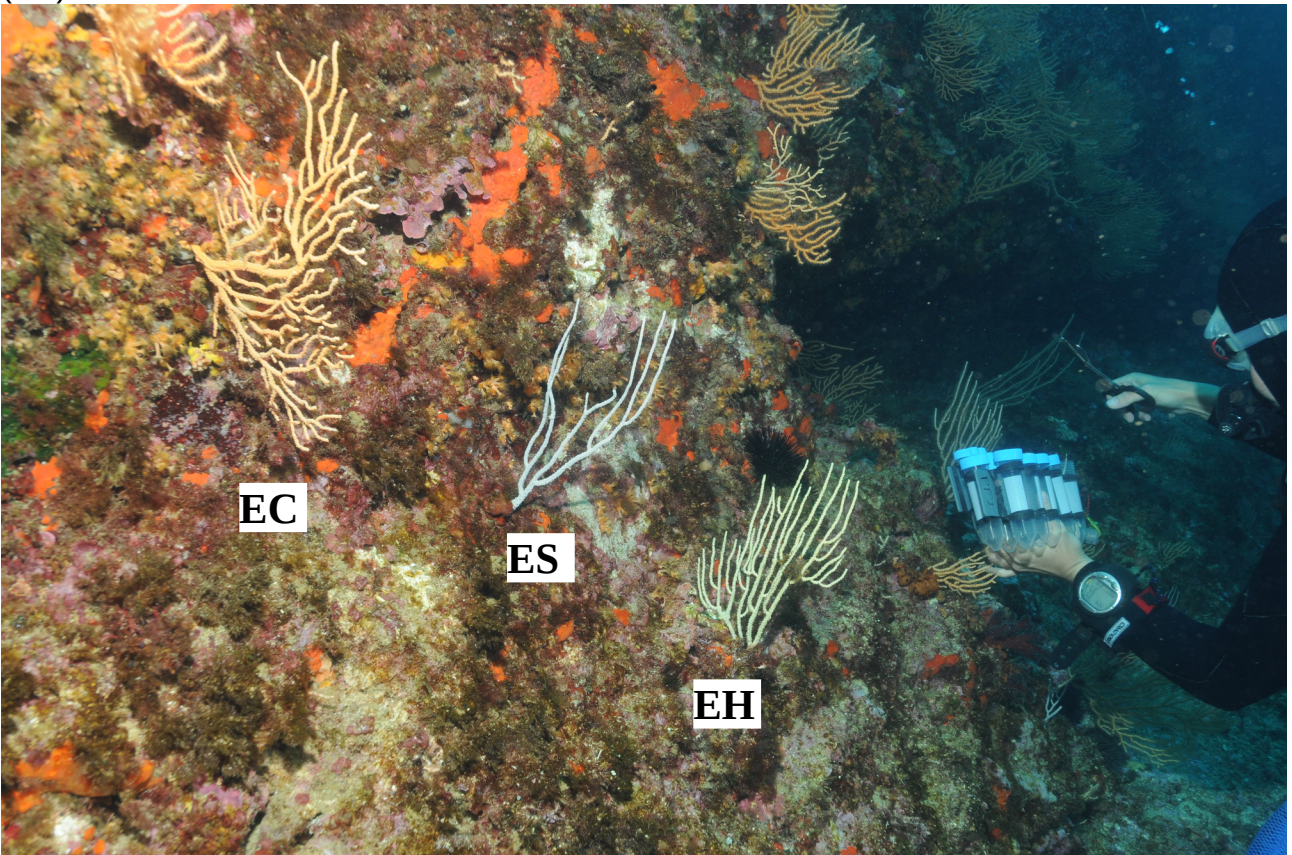
E) morphology of the colony EH-MFN-A (white, in the background) with white color as *E. singularis* but branching more similar to *E. cavolini*.
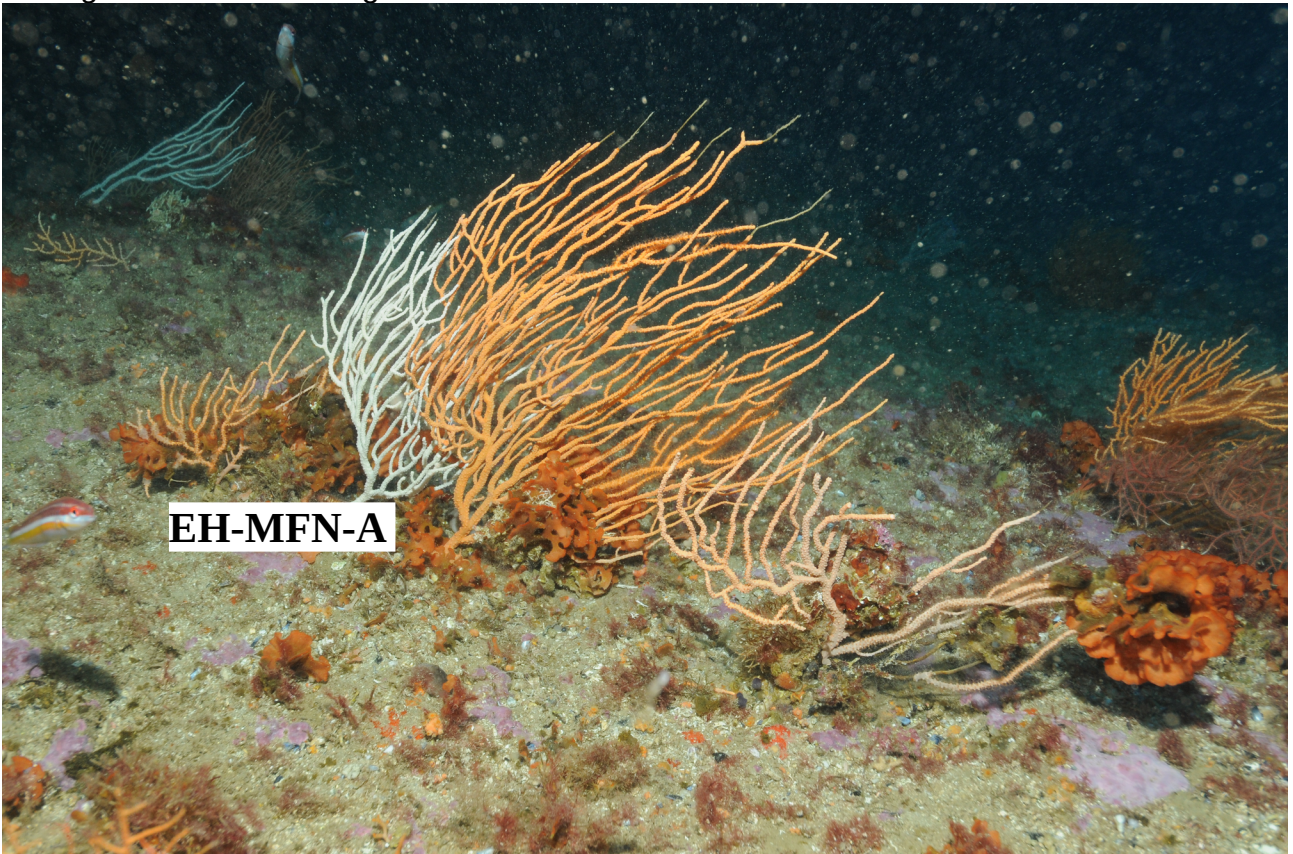
F) morphology of the colony EH-MFN-B with intermediate branching and color between *E. cavolini* and *E. singularis.*
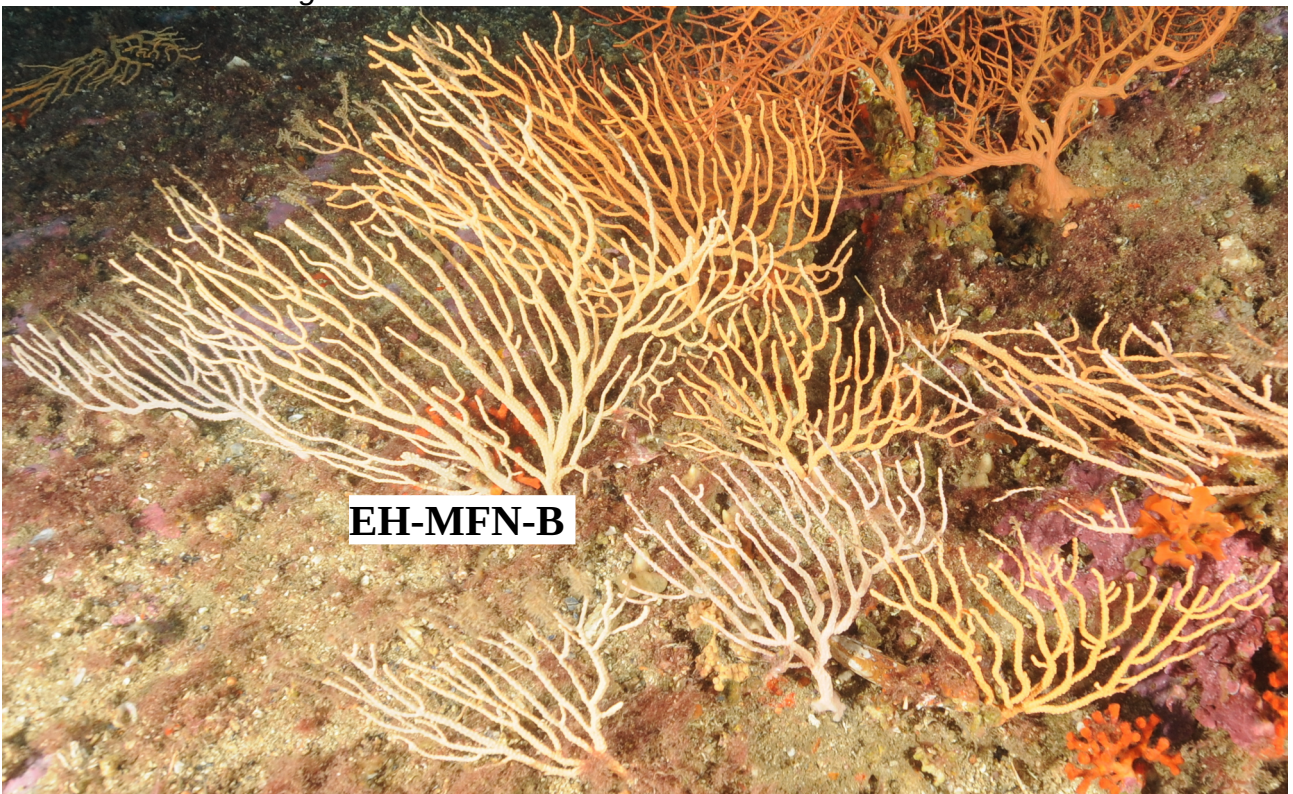
G) morphology of the colony EH-MFN-E with intermediate branching and color between *E. cavolini* and *E. singularis.*
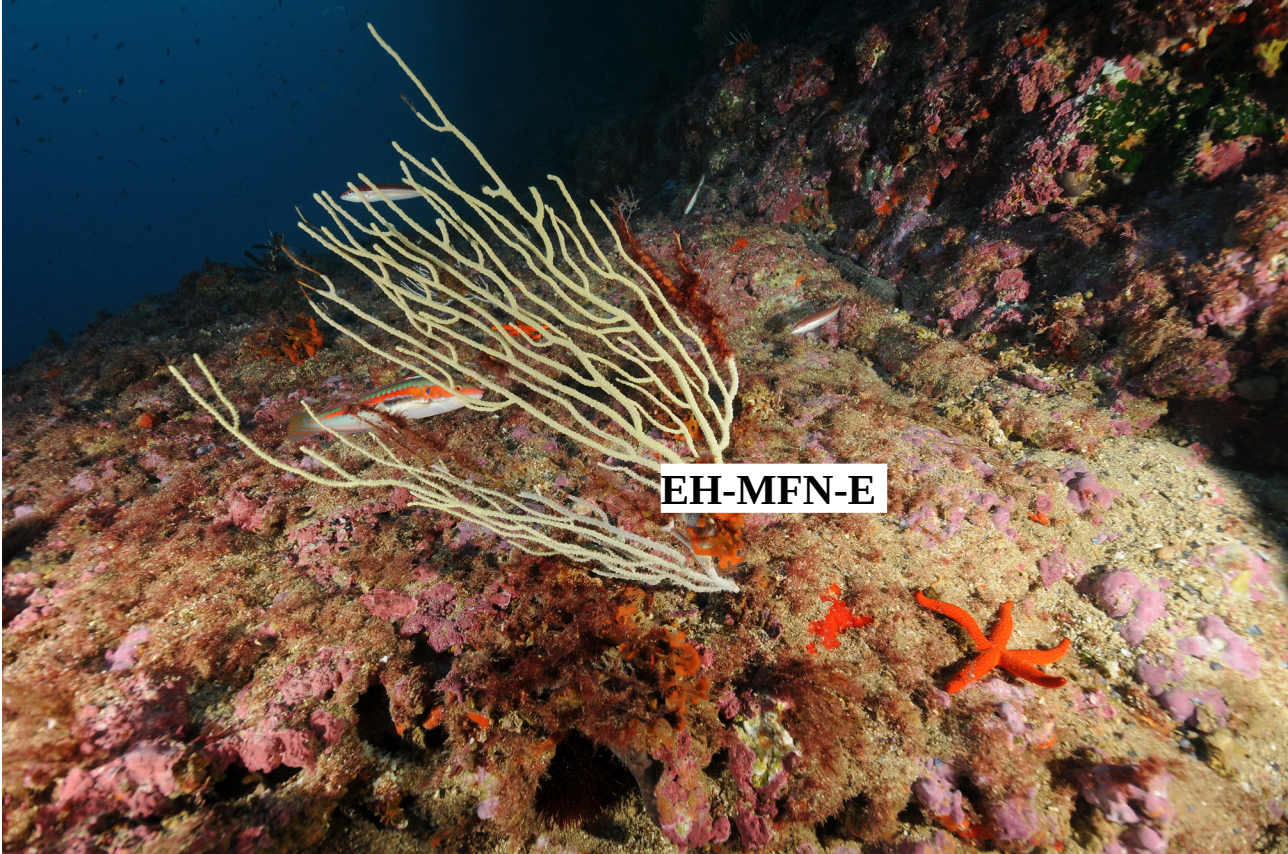
Figure S2: map of sampling sites for RAD sequencing in the area of Marseille. The symbols present the different samples: EC E. cavolini, ES E. singularis, EV E. verrucosa, HY hybrids. The three letters correspond to the codes of the sampling. The maps have been produced with the marmap R package (Pante & Simon-Bouhet, 2013) and following the tutorial of Krueger-Hadfield (2015).
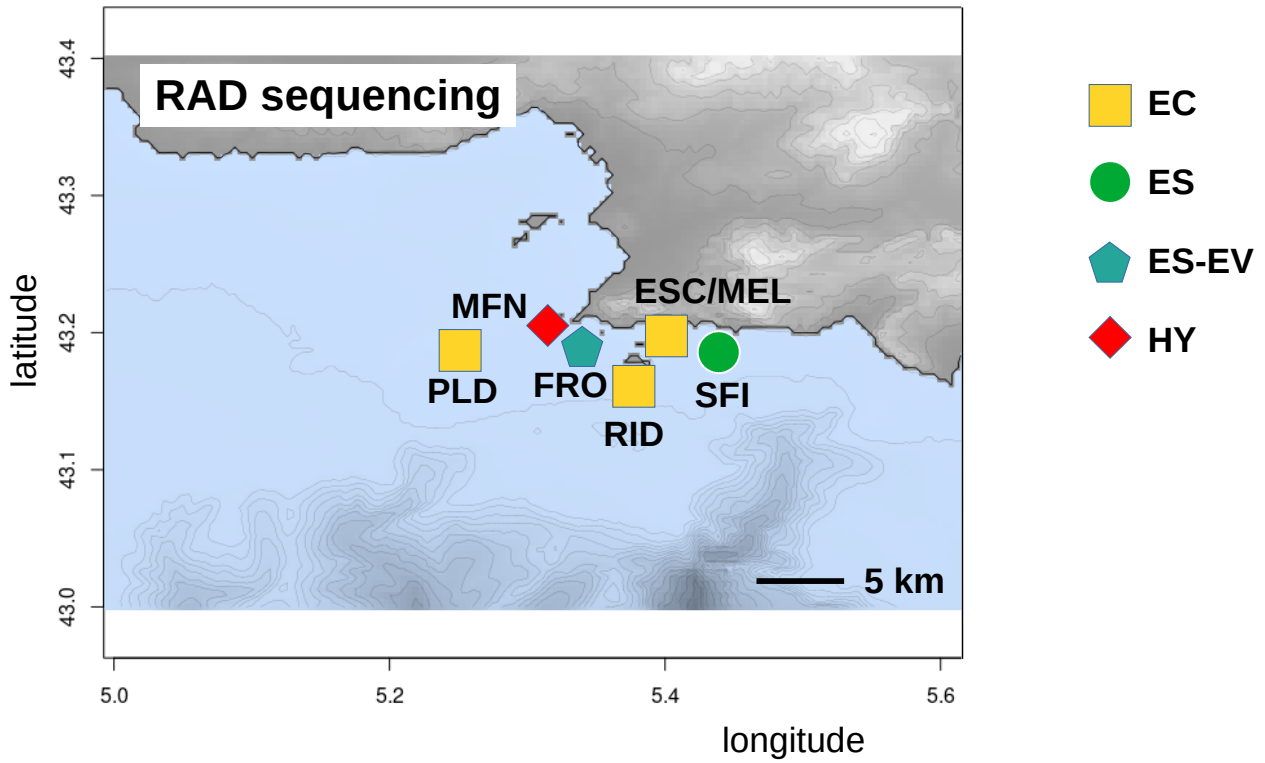
Figure S3: phylogenetic relationships among *Eunicella* species. The phylogenetic reconstruction has been performed with mitochondrial MutS sequences obtained from Genbank, with a search focused on *Eunicella* species. Sequences from the *Complexum* and *Swiftia* genera have been retained on the basis of a Blast search with the MutS sequence of *E. cavolini*, and according to the current systematics of octocorals (McFadden et al., 2022). The sequences corresponding to our three focal species come from previous studies and do not correspond to specimens sampled for the present study. The sequences have been edited with ugene (Okonechnikov et al., 2012). The phylogenetic reconstructions have been performed with the Maximum-Likelihood (ML) approach of IQ-TREE 2.1.1 (Nguyen et al., 2015). We used the ModelFinder option (Kalyaanamoorthy et al., 2017), and robustness was evaluated with 1000 ultrafast bootstraps (Hoang et al., 2018). The tree has been visualized with FigTree 1.4.4 (Rambaut, 2006) and was rooted with *Swiftia simplex* as outgroup. The numbers to the left of the nodes indicate the percentages of bootsraps. The Genbank accession numbers are listed in table S1.

References:

Hoang, D. T., Chernomor, O., Von Haeseler, A., Minh, B. Q., & Vinh, L. S. (2018). UFBoot2: Improving the ultrafast bootstrap approximation. *Molecular Biology and Evolution*, *35*(2), 518–522.

Kalyaanamoorthy, S., Minh, B. Q., Wong, T. K. F., von Haeseler, A., & Jermiin, L. S. (2017). ModelFinder: Fast model selection for accurate phylogenetic estimates. *Nature Methods*, *14*(6), 587–589. https://doi.org/10.1038/nmeth.4285

McFadden, C. S., van Ofwegen, L. P., & Quattrini, A. M. (2022). Revisionary systematics of Octocorallia (Cnidaria: Anthozoa) guided by phylogenomics. *Bulletin of the Society of Systematic Biologists*, *1*(3).

Nguyen, L.-T., Schmidt, H. A., von Haeseler, A., & Minh, B. Q. (2015). IQ-TREE: A Fast and Effective Stochastic Algorithm for Estimating Maximum-Likelihood Phylogenies. *Molecular Biology and Evolution*, *32*(1), 268–274. https://doi.org/10.1093/molbev/msu300

Okonechnikov, K., Golosova, O., Fursov, M., & Ugene Team. (2012). Unipro UGENE: a unified bioinformatics toolkit. *Bioinformatics*, *28*(8), 1166–1167.

Rambaut, A. (2006). *FigTREE v1.4*. University of Edinburgh. http://tree.bio.ed.ac.uk/software/figtree/
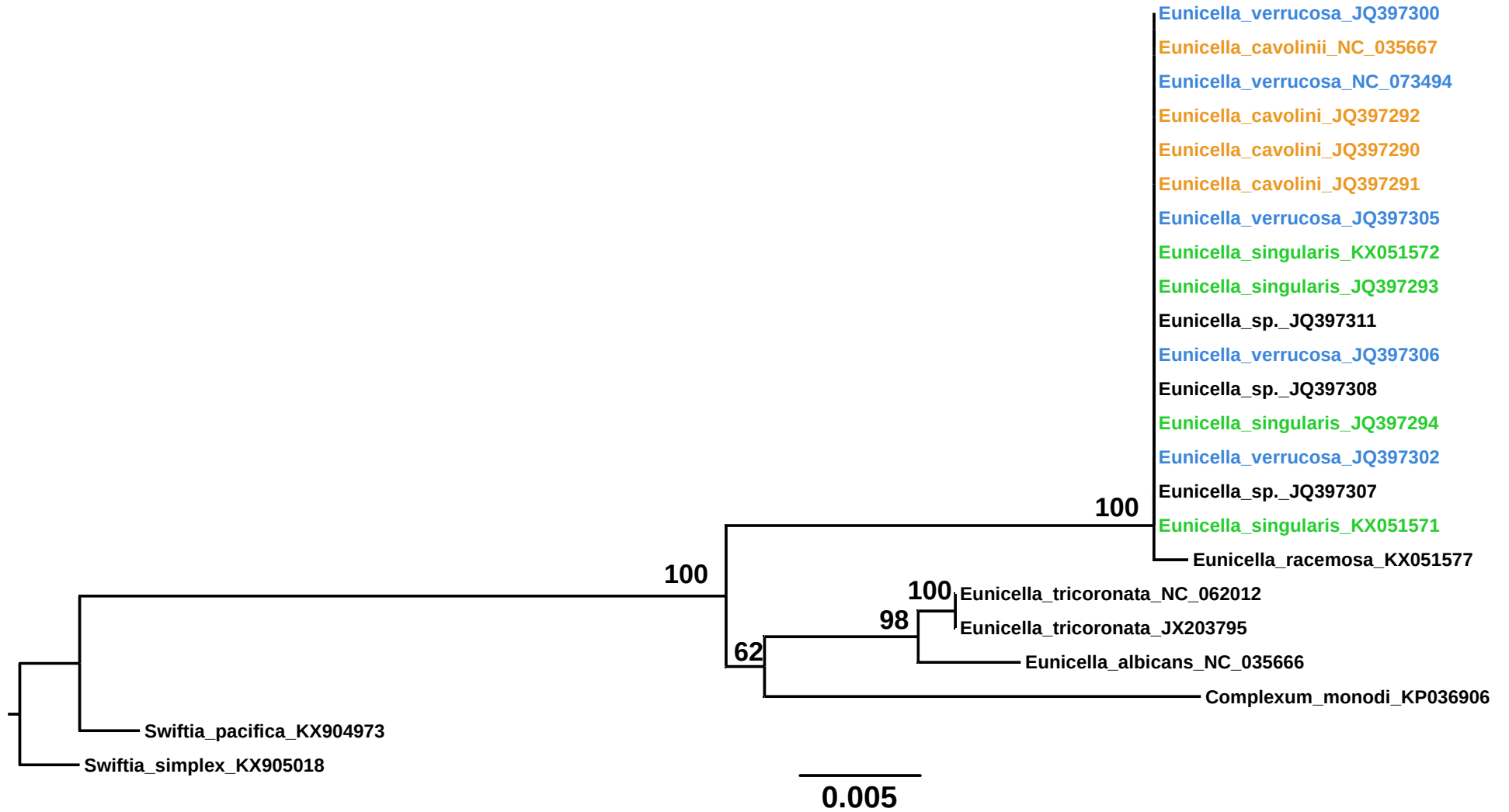
Figure S4: schematic representation of the four speciation scenarios tested with DILS (adapted from Roux *et al.*, 2016). The green background indicates the species history, and the red lines show an example of the history of one gene. All scenarios correspond to a divergence from an ancestral population but differ by the possibility and timing of migration (i.e. gene flow) versus isolation (no gene flow). Among these four scenarios, only isolation / migration and secondary contact imply current gene flow among species. In the strict isolation scenario, there is no gene flow after divergence, whereas in the ancestral migration scenario, divergence is followed by a period of gene flow, then by isolation. For simplicity we did not add here the possibility of variation in effective sizes (NA and NB). DILS also allowed to test genomic heterogeneity in gene flow, which corresponds to differences in probability of gene flow among loci.

Strict isolation

Isolation / migration

Ancestral migration

Secondary contact

ancestral population N_{anc}

T_{DIV}

past

present

species A N_A species B N_B

T_{AM}

T_{SC}
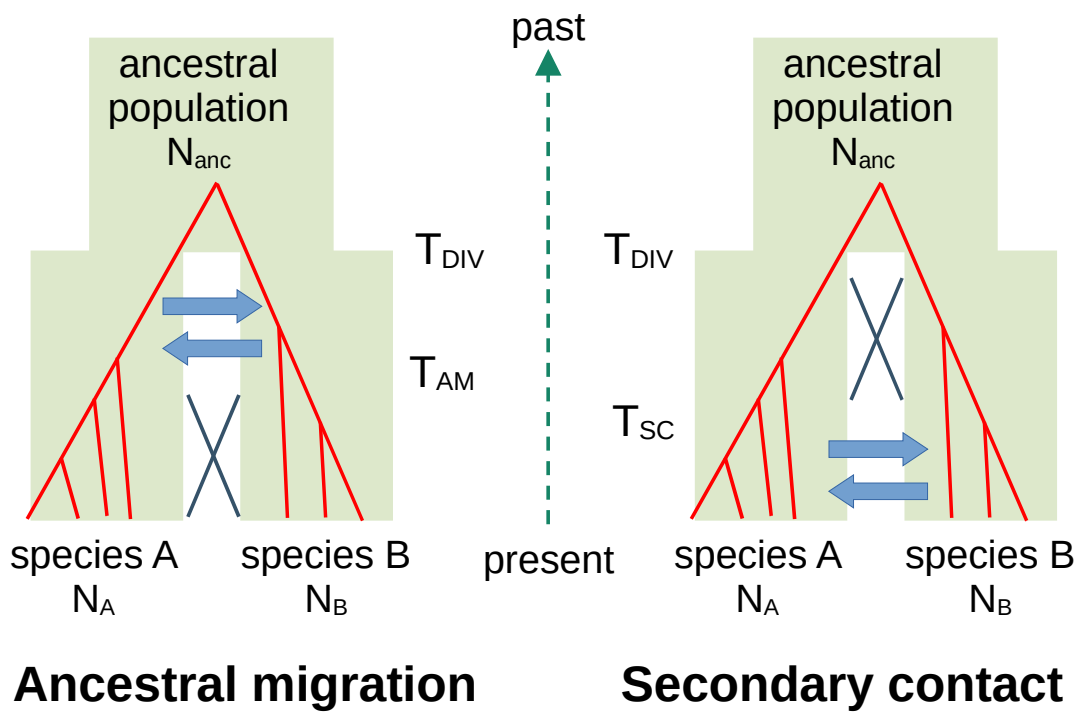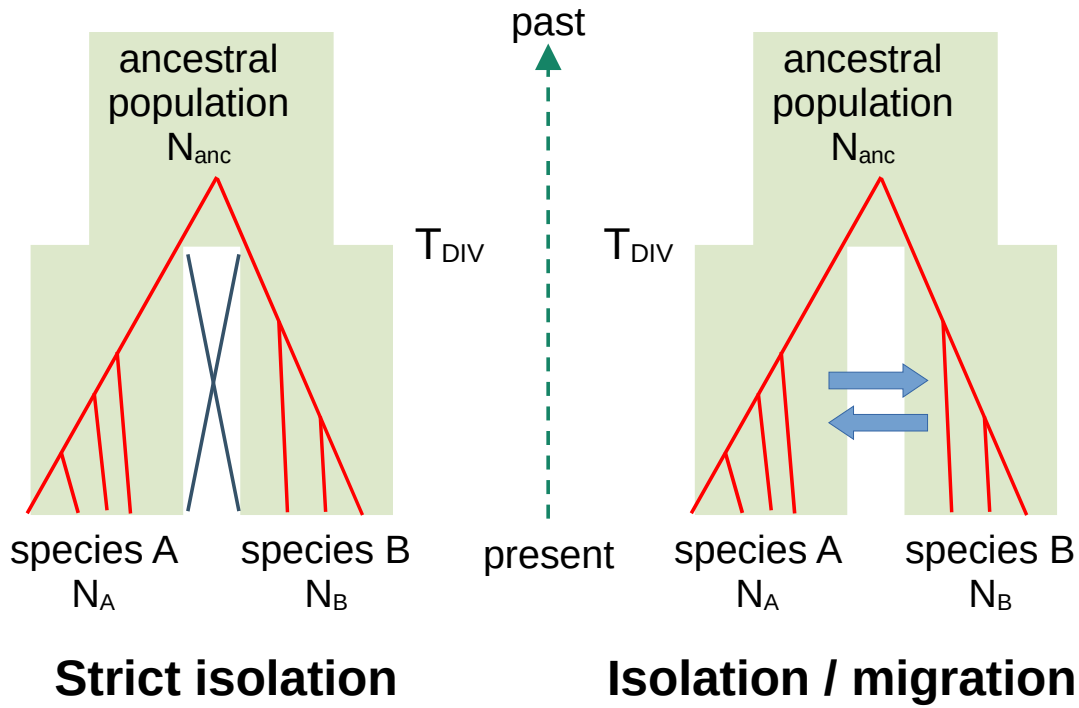
✕ Isolation (no gene flow)

⇄ Gene flow

T_{DIV} divergence time

T_{AM} end of ancestral migration

T_{SC} time of secondary contact

Figure S5: barplots of coancestry coefficients inferred with the LEA R package for K = 3 with RAD sequencing with the four assembly strategies. The red asterisks indicate the individuals used as prior for parental status in the NewHybrids analysis. For clarity reasons, the precise results of the NewHybrids analysis are not indicated here but they can be found in Table 1.

de novo

genome *E. cavolini*

genome *E. singularis*

genome *E. verrucosa*

hybr. | *E. cavolini* | hybr. | *E. singularis* | *E. verru-cosa*

Figure S6: Principal Component Analysis based A) on the RAD_denovo dataset; B) on the RAD_EC dataset; C) on the RAD_ES dataset; D) on the RAD_EV dataset. For each analysis we present a) the plots on axes 1 and 2, and b) on axes 3 and 4. E) on transcriptome data, axes 3 and 4.

A) RAD sequencing, de novo assembly; axis 1 represents 21% of the variance, axis 2 represents 10.2% of the variance, axis 3 represents 3% of the variance, axis 4 represents 3% of the variance.

a)
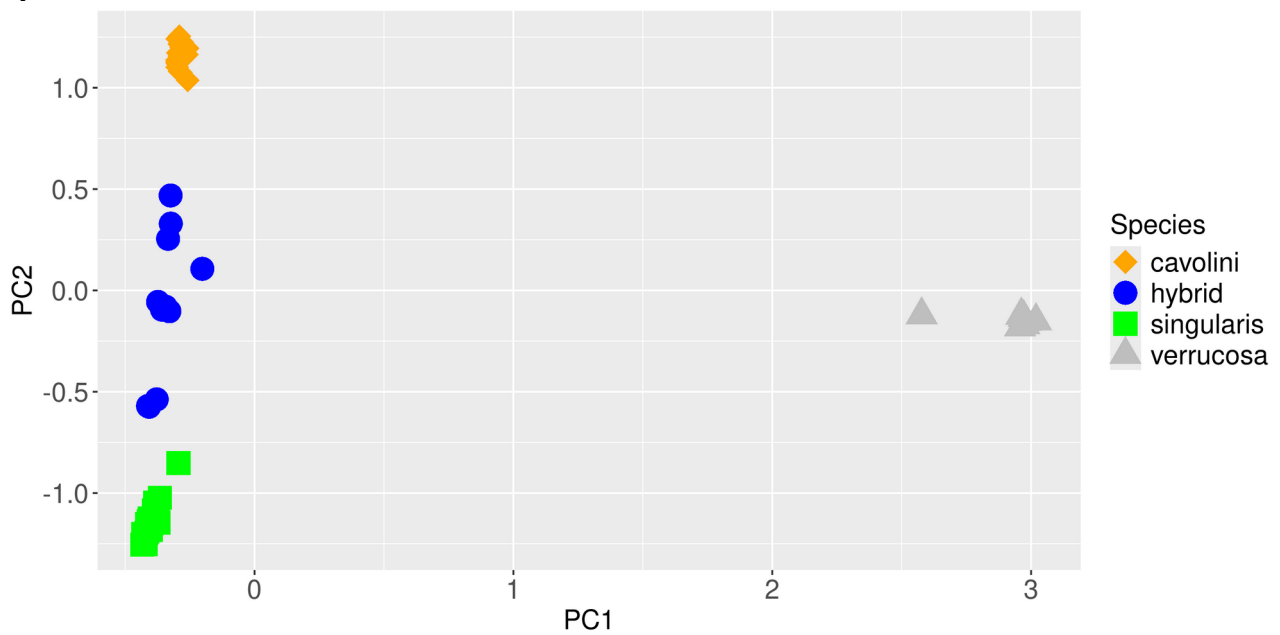
b)
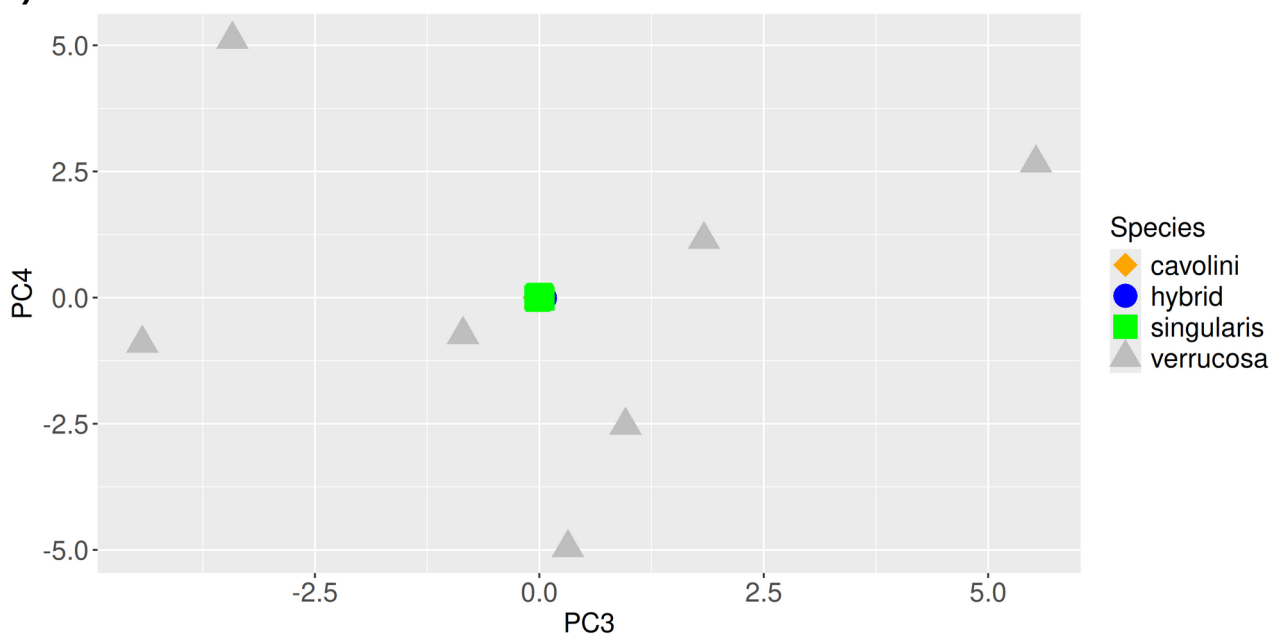
B) RAD sequencing, assembly on *E. cavolini* genome; axis 1 represents 18.7% of the variance, axis 2 represents 10.2% of the variance, axis 3 represents 2.9% of the variance, axis 4 represents 2.8% of the variance.

a)
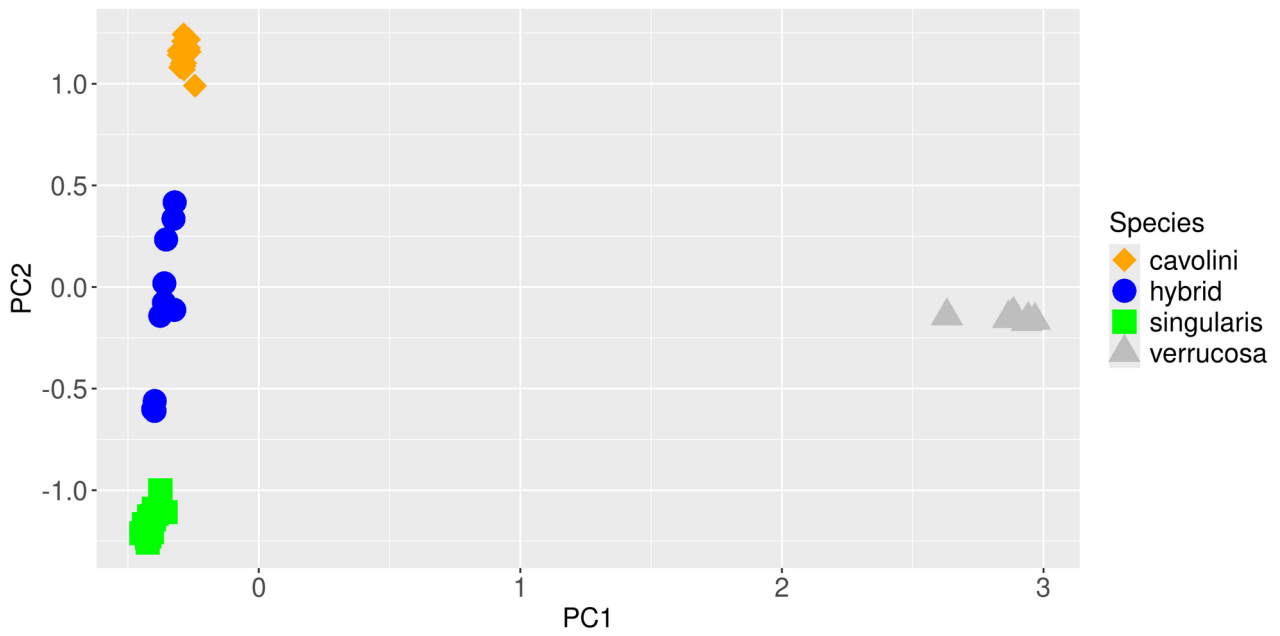
b)
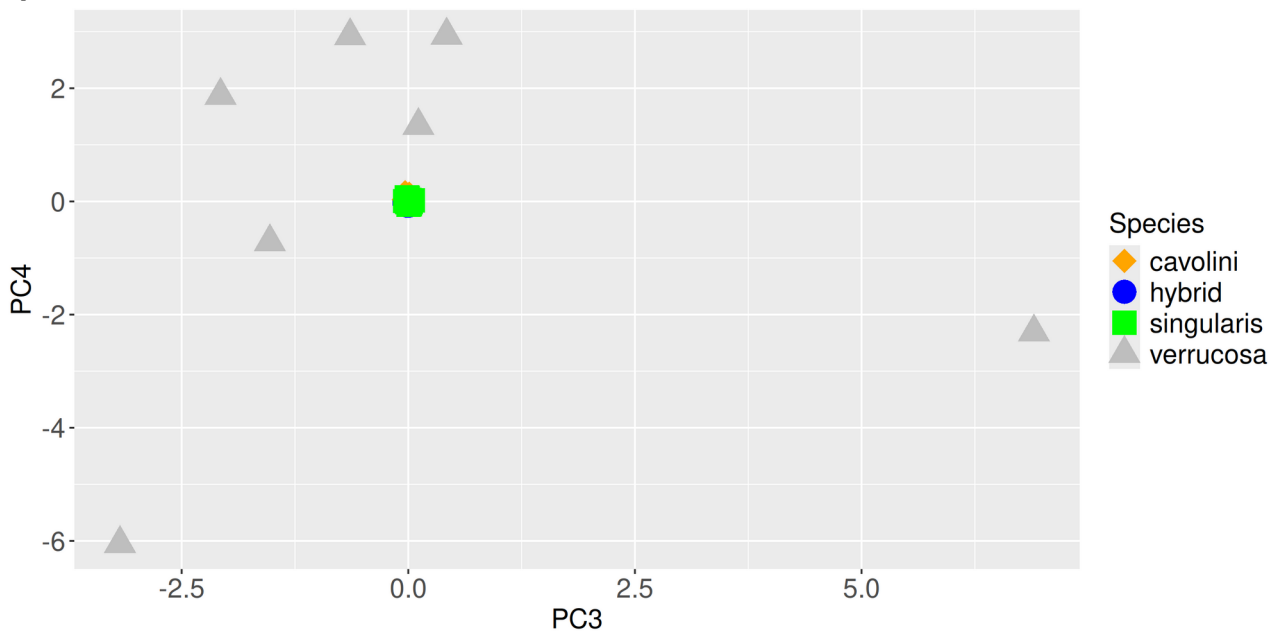
C) RAD sequencing, assembly on *E. singularis* genome; axis 1 represents 18.8% of the variance, axis 2 represents 9.8% of the variance, axis 3 represents 2.8% of the variance, axis 4 represents 2.7% of the variance.

a)
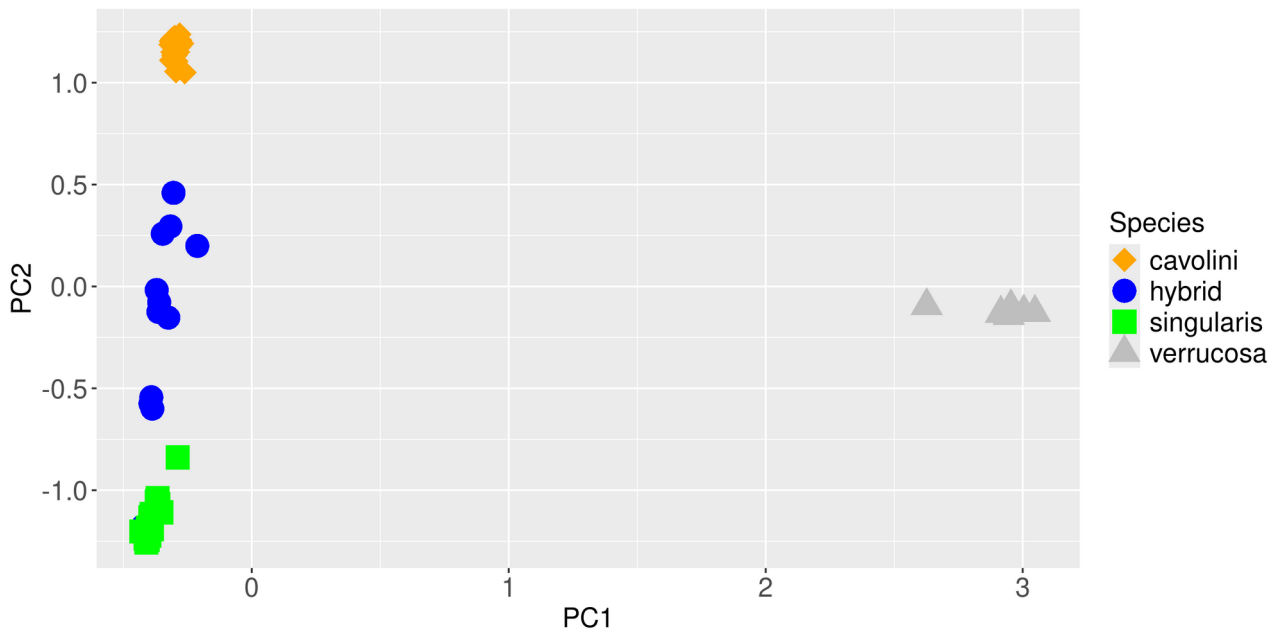
b)
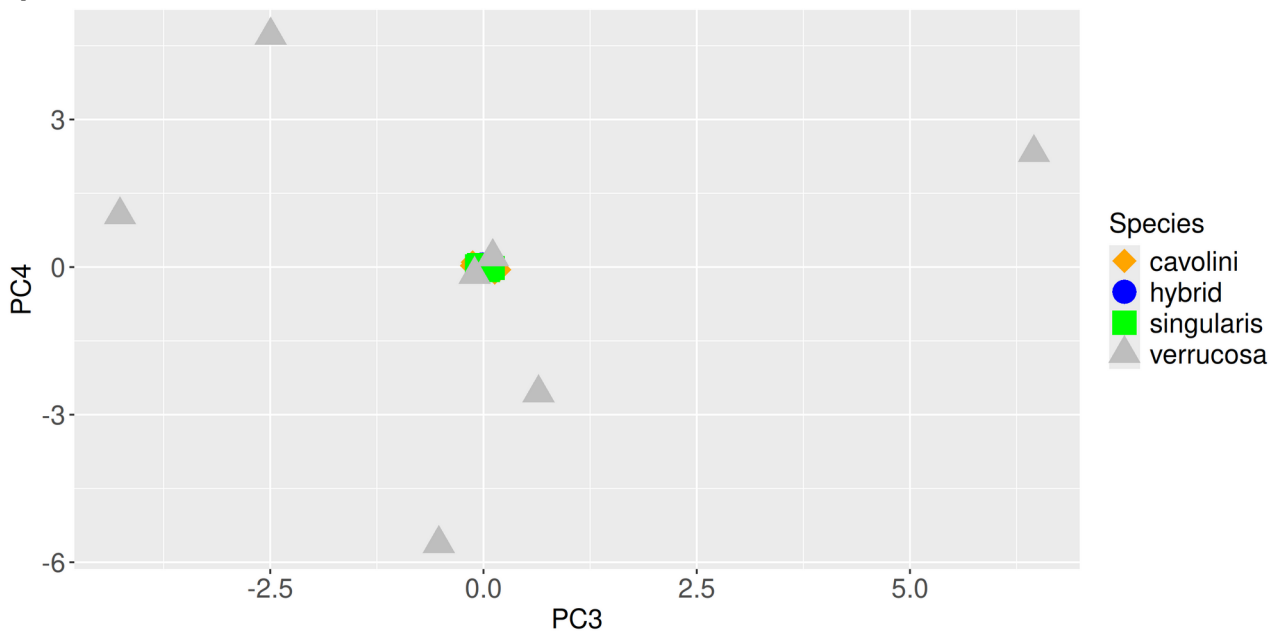
D) RAD sequencing, assembly on *E. verrucosa* genome; axis 1 represents 14.1% of the variance, axis 2 represents 7.1% of the variance, axis 3 represents 2.8% of the variance, axis 4 represents 2.6% of the variance.

a)
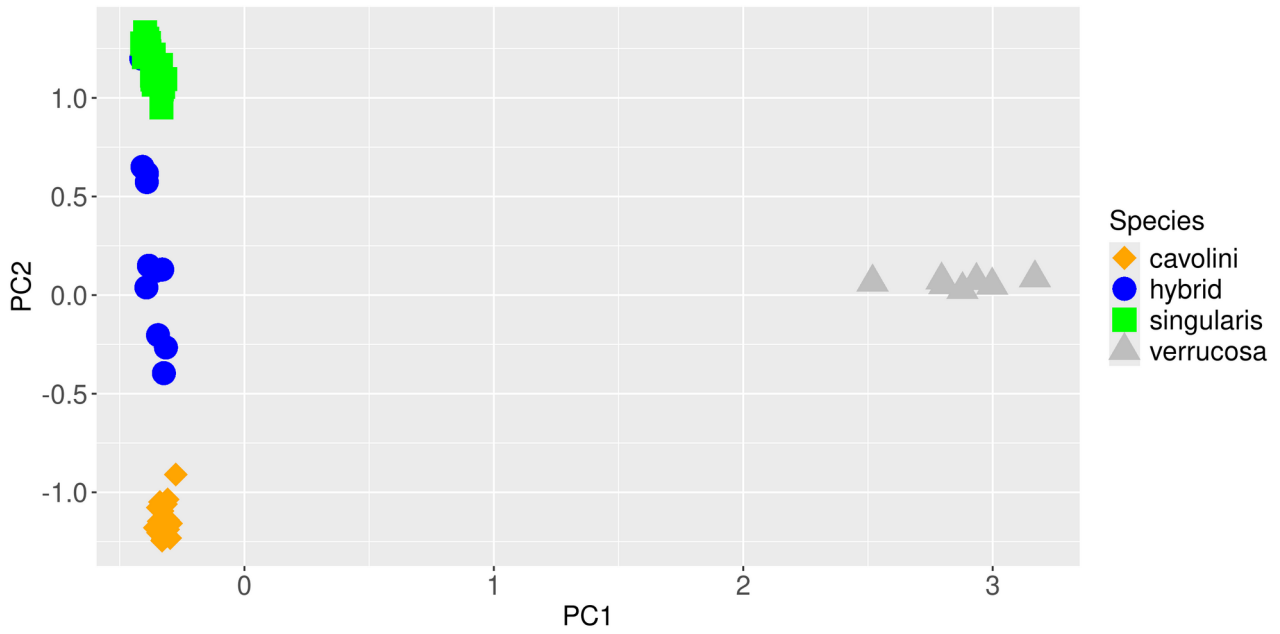
b)
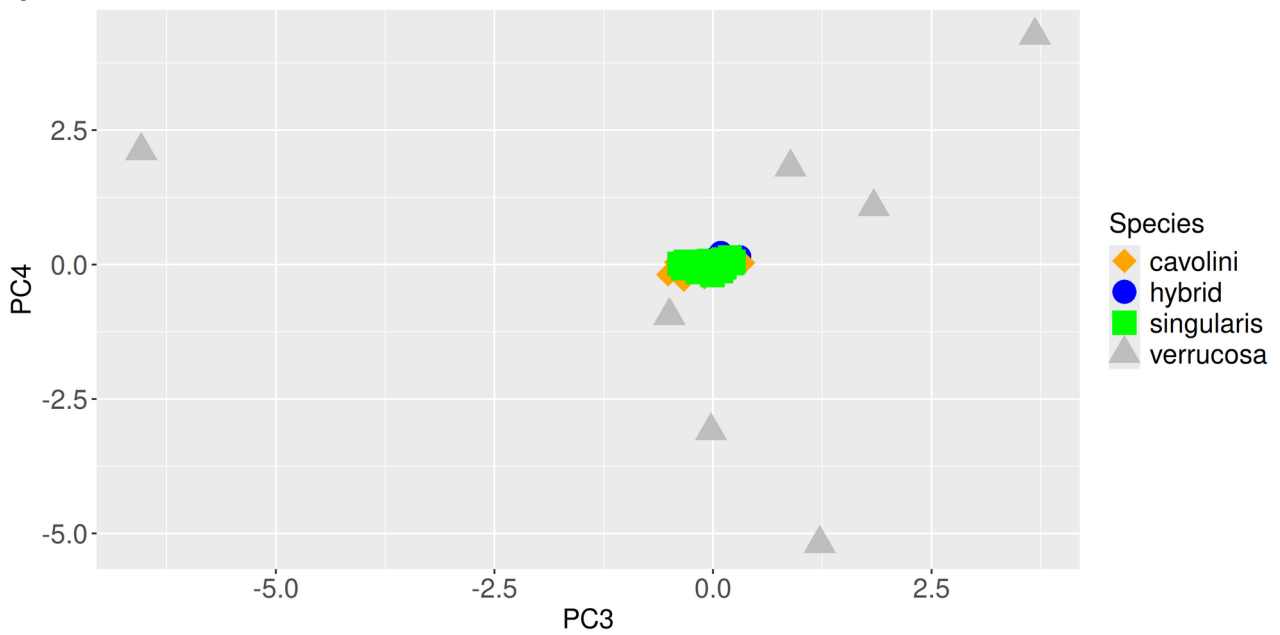
E) transcriptome data; axis 3 represents 6.1% of the variance, axis 4 represents 4.2% of the variance. The two points on the right side (high positive values on axis 3) corresponds to the two *E. cavolini* samples from the ANB site in Algeria. The projection on axes 1 and 2 is presented in the main text (Figure 4).
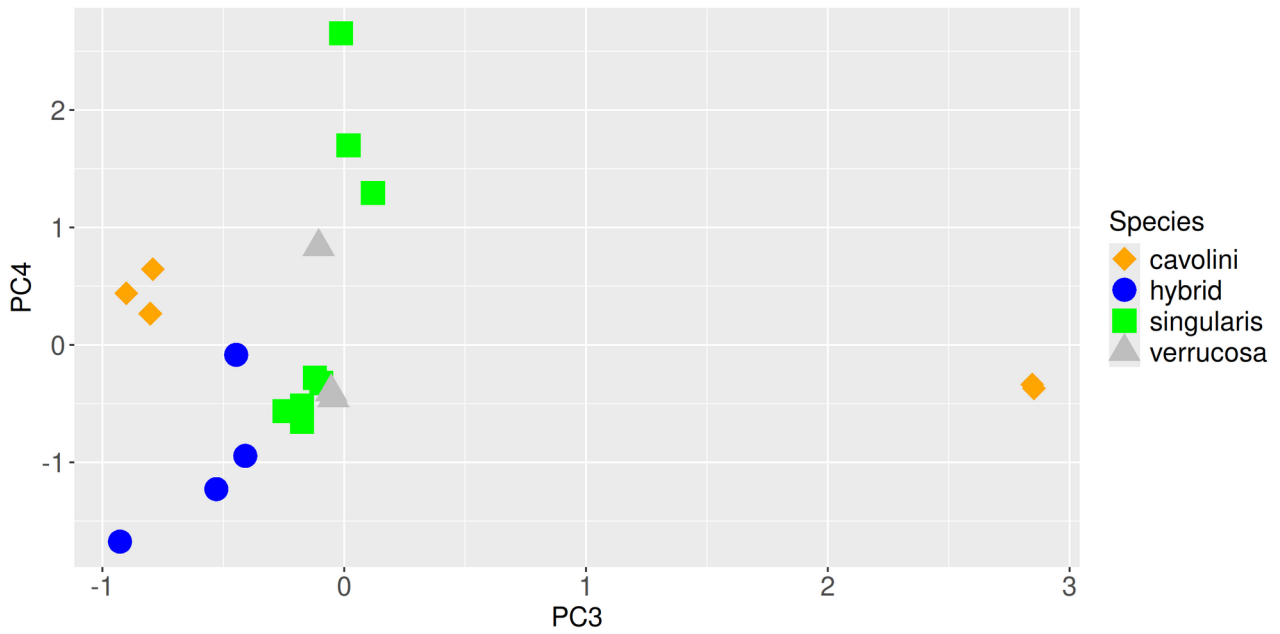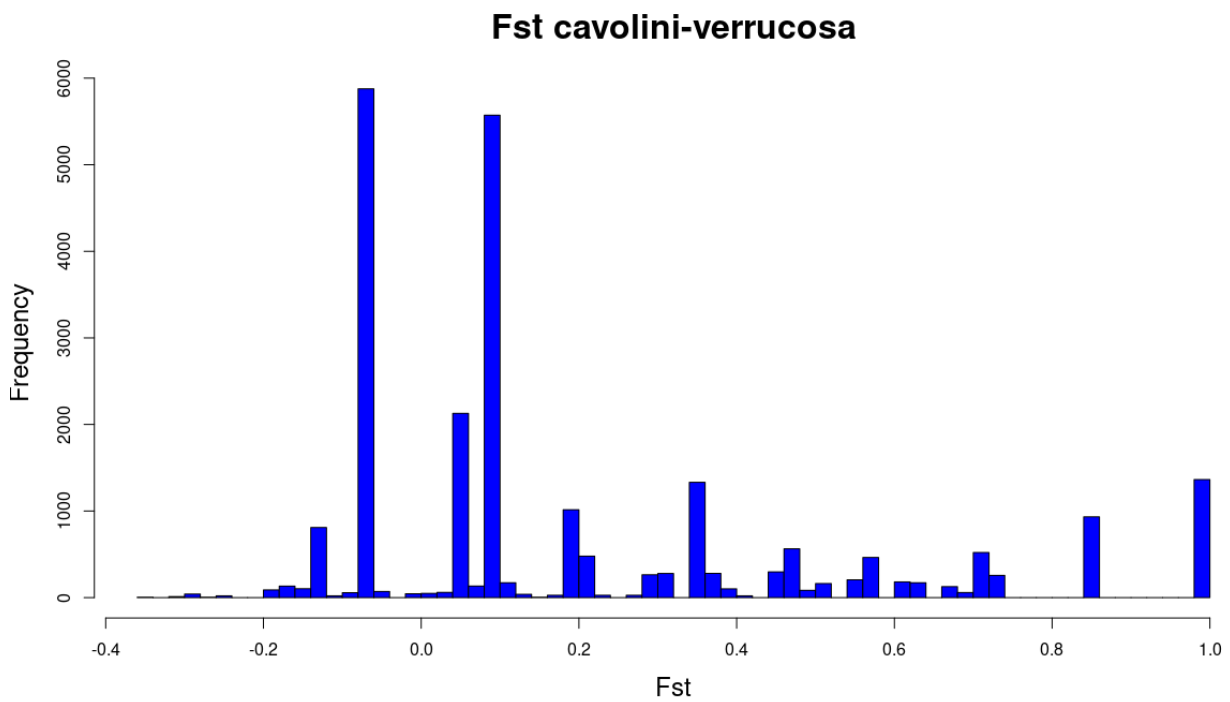
Figure S7: distribution of F_{ST} estimates over loci, for the pairwise comparisons among the three species, with the exclusion of potential hybrids.

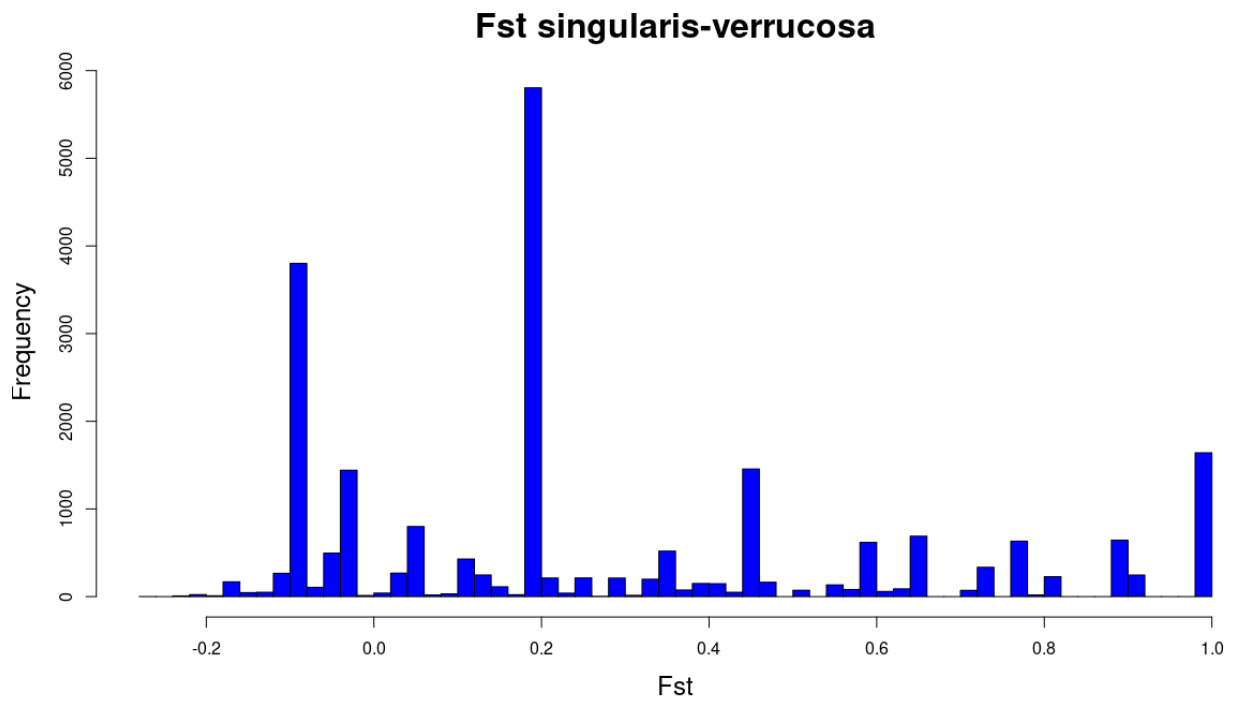A) comparison between *E. cavolini* and *E. singularis*

Fst cavolini-singularis
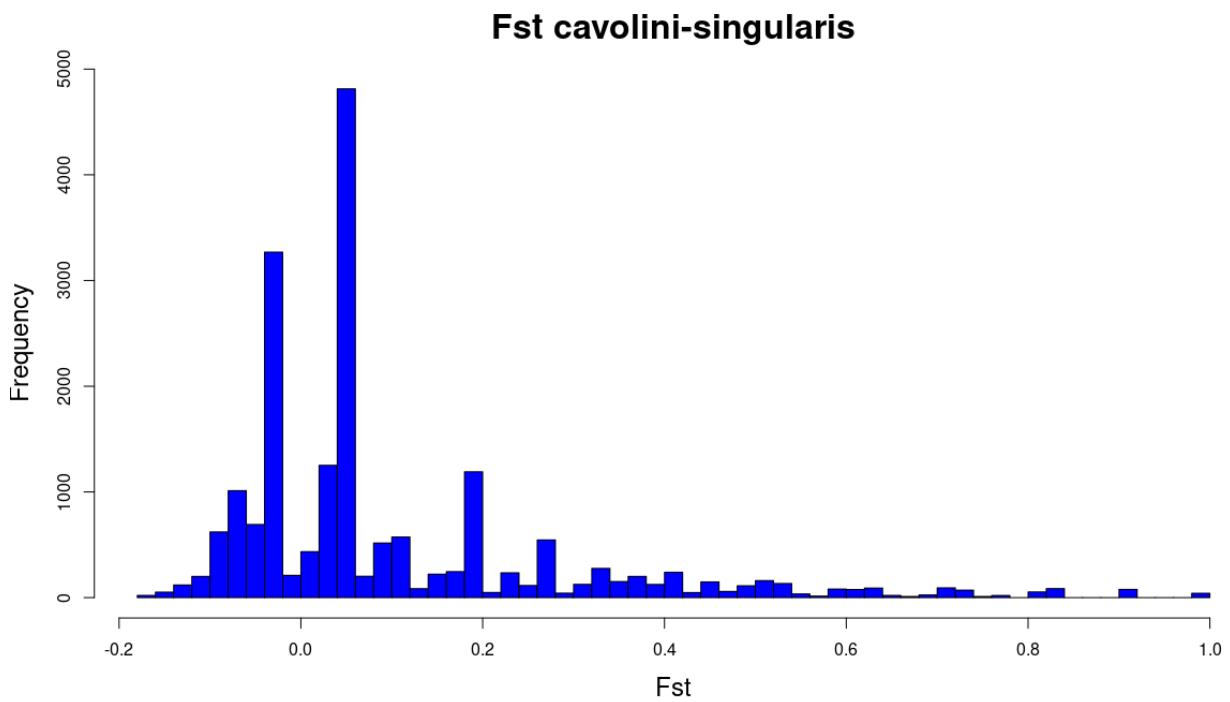
B) comparison between *E. cavolini* and *E. verrucosa*

Fst cavolini-verrucosa

C) comparison between *E.singularis* and *E. verrucosa*

Fst singularis-verrucosa

Figure S8: result of the cross-entropy analysis with the LEA R package for transcriptome data